

Chapter 2

Nanotechnology

2.1 Introduction to Nanotechnologies and Nanopackaging

Nanotechnology is the creation of functional materials, devices, and systems through control of matter on the nanometer length scale (<100 nm) and exploitation of novel phenomena and properties (physical, chemical, biological, mechanical, electrical, etc.) at that length scale.

Nanoelectronics refer to the use of nanotechnology on electronic components. Nanoelectronics hold the promise of making computer processors more powerful than is possible with conventional semiconductor fabrication techniques. A number of approaches are currently being researched, including new forms of nanolithography, as well as the use of nanomaterials such as nanowires or small molecules in place of traditional CMOS components. Field-effect transistors have been made using both semiconducting carbon nanotubes [1] and heterostructured semiconductor nanowires [2].

Single-molecule devices are another possibility. These schemes would make heavy use of molecular self-assembly, designing the device components to construct a larger structure or even a complete system on their own. This can be very useful for reconfigurable computing.

Molecular electronics [3] is a new technology which is still in its infancy, but also brings hope for truly atomic scale electronic systems in the future. One of the more promising applications of molecular electronics was proposed by the IBM researcher Ari Aviram and the theoretical chemist Mark Ratner of North Western University in their 1974 and 1988 papers *Molecules for Memory, Logic and Amplification*, respectively [4, 5]. This is one of many possible ways in which a molecular-level diode/transistor might be synthesized by organic chemistry. A model system was proposed with a spiro carbon structure giving a molecular diode about half a nanometer across which could be connected by polythiophene

molecular wires. Theoretical calculations showed the design to be sound in principle and there is still hope that such a system can be made to work.

Nanopackaging, i.e., the application of nanotechnologies to electronics packaging, is being explored to enhance performance and reliability electronics packages. Nanotechnology drivers are the varied ways in which materials properties change at small dimensions, and these properties can be put to work to solve past packaging problems and to develop new approaches to future nanoelectronics packaging issues. Electron transport mechanisms at small dimensions include ballistic transport where the transport of electronic signal without generating any measurable heat, severe mean free path restrictions in very small nanoparticles, various forms of electron tunneling, electron hopping mechanisms, and more.

In addition, candidate next-generation nanoelectronics technologies (e.g., single-electron transistors, quantum automata, molecular electronics) are generally hyper-sensitive to dimensional change, if based on quantum mechanical electron tunneling, and appropriate packaging will be essential to the success or failure of these technologies. Packaging strategies must therefore be developed in parallel with the basic nanoelectronics device technologies in order to make informed decisions as to their commercial viabilities [6].

2.2 Nanoparticles

2.2.1 Introduction

The transition from micro-particles to nanoparticles can lead to a number of changes in physical properties. Two of the major factors are the increase in surface area to volume ratio and the size of particles moving into the realm where quantum effects predominate.

The increase of surface-area-to-volume ratio, which is a gradual progression with particles getting smaller, leads to an increasing dominance of the behavior of the atoms on the surface of the particles over that of those in the interior of the particle. This affects both the properties of a particle in isolation and its interaction with other materials. The large surface area results in lots of interactions between intermixed materials in nanocomposites, leading to special properties.

Once particles become small enough they start to exhibit quantum mechanical behavior. The property of quantum dots is a case in point, whereas these are sometimes called artificial atoms because free electrons

in them start to behave in a way similar to electrons bound by atoms in that they can only occupy certain permitted energy states.

Additionally, the fact that nanoparticles have dimensions below the critical wavelength of light make them transparent, a property that makes them very attractive for applications in packaging, cosmetics, and coatings.

2.2.2 Nanoparticle Fabrication

The nanoparticle fabrication technique to be selected depends primarily on the intended functions. Usually, chemical reduction [7–12] and physical method [13] have been developed to synthesize bimetallic nanoparticles. The chemical reduction method for the preparation of bimetallic nanoparticles can be divided into two groups: one is the co-reduction of two different kinds of metal salts. For instance, Ag/Au alloy, El-Sayed and Murphy used simultaneous reduction of silver and gold salts to form Ag/Au alloy nanoparticles with size of 18 nm and less than 10 nm, respectively. Chen et al. [14] and Zhang et al. [15] used laser irradiation of silver–gold colloidal mixture to synthesize Ag/Au alloy nanoparticles. The other method is the successive reduction of two-metal salts, which is usually carried out to prepare a core–shell structure of bimetallic nanoparticles. Mandal et al. [16] used seed-mediated techniques to synthesize core-shell type Ag/Au bimetallic nanoparticles. For the physical method, nanoparticles can be made directly from the bulk materials. Compared to the chemical reduction method, the physical method renders higher yield. Particles produced by this method are usually quite large and have a wide distribution of particle size.

Noble metal nanoparticles, for example, have been fabricated by an eco-friendly ultrasonic processing technique. Beveridge and co-workers [17, 18] have demonstrated that gold particles of nanoscale dimensions may be readily precipitated within bacterial cells by incubation of the cells with Au^{3+} ions. Klaus et al. [19–21] have shown that the bacteria *Pseudomonas stutzeri* AG259 isolated from a silver mine, when placed in a concentrated aqueous solution of AgNO_3 , resulted in the reduction of the Ag^+ ions and formation of silver nanoparticles of well-defined size and distinct morphology within the periplasmic space of the bacteria. Taking this approach a step further, they showed that biocomposites of nanocrystalline silver and the bacteria may be thermally treated to yield a carbonaceous (cermet) nano-material with interesting optical properties for potential application in functional thin-film coatings [21]. The exact reaction mechanism leading to the formation of silver nanoparticles by this species of silver-resistant bacteria was not clear. In an interesting recent study, Nair and Pradeep [22] have demonstrated that bacteria not normally exposed to

large concentrations of metal ions may also be used to grow nanoparticles. Nair and Pradeep have shown that *Lactobacillus* strains present in buttermilk, when challenged with silver and gold ions, resulted in the large-scale production of metal nanoparticles within the bacterial cells. They also showed that exposure of lactic acid bacteria present in the whey of buttermilk to mixtures of gold and silver ions could be used to grow nanoparticles of alloys of gold and silver [22]. Recently, Jose-Yacaman and co-workers [23, 24] have shown that gold and silver nanoparticles may be synthesized in live alfalfa plants by gold and silver uptake from solid media.

A precursor may be used, e.g., AgNO_3 for Ag nanoparticles, and there are techniques to control the particle shapes, e.g., spherical, cubic, or wires [6, 25]. Nanoparticles tend to agglomerate, and so the crucial step is often the use of a dispersant to counter this tendency [26, 27]. The thermal or sputter evaporation of metals and condensation on an insulating substrate will also yield a surface distribution of nanoparticles [28–31].

The enhanced chemical activities of nanoparticles, which make them effective as catalysts, are due to the high surface area-to-volume ratio, and hence to the high proportion of unsatisfied chemical bonds. In addition, other physical property changes include the following:

- **Melting point depression:** The melting points of small metal nanoparticles drop significantly with decreasing size at dimensions under 5 nm [26].
- **Sintering:** The thermally activated surface self-diffusion process drives net diffusion away from convex surfaces of high curvature, and into concave surfaces, yielding low-temperature bonding between nanoparticles in contact.
- **Coulomb block, or blockade:** An external field or thermal source of electrostatic energy is required to charge an individual nanoparticle; this effect is the basis of single-electron transistor operation [32].
- **Single grain structures,** such as nanoparticles, may achieve theoretical maximum mechanical strengths [33].
- **Nanoparticles** one to two orders smaller than the wavelength of visible light provide unique optical scattering properties [34] and absorption peaks which “color” thin films or suspensions of such nanoparticles.

2.2.3 Nanoparticle Applications

Embedded passive components are seen to be the solution to the problem of high proportions of PWB (printed wiring board) surface space being occupied by discrete passives. The “cermet” (ceramic–metal) resistors used in specialized on-chip applications are adaptable to the embedded PWB role. The structure consists of metallic nanoparticles embedded in a

dielectric (or polymer) with electron tunneling as the transport mechanism between particles. At low fields, the coulomb block array is randomly charged by thermal energy, giving a high negative temperature coefficient of resistance (TCR), offset by the inclusion of positive TCR metallic paths. Examples of structure-related properties are provided for the $\text{Cr}_x(\text{SiO})_{1-x}$ and $(\text{Cr}_x\text{Si}_{1-x})_{1-y}\text{N}_y$ systems.

High dielectric constant, k , and minimal thickness are required for embedded capacitors. The former requirement is met by the inclusion of high dielectric constant particulates, and the latter requirement suggests nanoparticles, e.g., barium titanate, or metals. Nanoparticle surface energies must be reduced to avoid aggregation [27]. The target k is 50–200; $k \sim 150$ has been achieved with metal nanoparticles at the expense of high leakage (dielectric loss), since this is a similar structure to the cermet resistor, albeit at lower metallic load. An ultra-high k epoxy/carbon black polymeric composite with k in excess of 13,000 has been reported by Xu and Wong [38], but the loss is quite high in 0.1. However, when the epoxy matrix resin with a loss of 0.02 was replaced with a BCB (benzocyclobutene) with a loss of 0.008, a much lower loss composite was achieved at ~ 0.06 . An alternative approach to leakage is to use aluminum particles, to take advantage of the native oxide coating [35], with $k \sim 160$ achieved [36]. Ag/Al mixtures have also been studied [37].

Note that thermally conductive materials have very similar structural requirements to the passive components, with metallic or SiC nanoparticles as fillers [38].

Inductive components are also required, especially for RF applications. Classical magnetism theory turns out to be inapplicable for nanograin dimensions less than the ferromagnetic exchange length (tens of nanometers) which can sustain high permeability and low coercivity.

The simple addition of nanoparticles to traditional isotropic electrically conductive adhesives (ICAs) filled with micron-sized Ag fillers in an epoxy matrix might be expected to lower resistivity by providing bridges between particles, but does not in fact improve conductance, due to mean free path restrictions and added interface resistances. The same principles limit the performance of alumina-loaded thermal composites [39]. The addition of silver nanoparticles does achieve dramatic reductions, however, by sintering wide-area contacts between flakes [40], a principle also applicable to micro-via fill in PWBs [41], which can also profitably use ICA materials. Nanoparticle filler sintering is the key step in any effective use of nanoparticles in these technologies and can also improve anisotropic conductive adhesive performance [42], aided by contact conductance enhancement by the addition of self-assembly molecular surface treatments [43, 44].

PWB surface electrical interconnect is achievable by screen or “ink-jet” printing of nanoscale metal colloids in suspension [45–48]. As above, electrical continuity is established by sintering Ag nanoparticles [49–52], which can also be used for die attach.

Fused silica fillers are added to flip chip underfills to reduce the coefficient of thermal expansion, and nanoparticles resist settling better [53] and scatter light less than larger fillers, permitting UV optical curing [54] and other advantages of optical transparency [55]. The higher viscosity of the nano-filled material can be reduced by silane surface treatments. Physical properties have been successfully modeled in terms of structural parameters. Nanoparticles with functionalized surfaces may be employed to increase the modulus, glass transition temperature (T_g), and dielectric property such as voltage endurance of polymer composites due to the strong interaction between the nanoparticles and the polymeric matrix and larger interaction zone [56, 57].

The addition of Pt, Ni, or Co nanoparticles to lead-free SnAg-based solder [58, 59] eliminates Kirkendall voids, reduces intermetallic compound (IMC) growth, and reduces IMC (intermetallic compound) grain sizes, significantly improving drop-test performance [60], promoting finer grain growth, increased creep resistance, and better contact wetting [61]. Nanoparticles in solder grain boundaries also inhibit grain-boundary sliding and thermo-mechanical fatigue.

2.3 Nano Solder Particles

Compared to micron-sized solder alloy particles, the nano solder particles potentially have the following advantages:

- ◆ Depression in melting temperature
 - Reduce processing temperature
 - Reduce thermal stresses on components and substrate during processing
- ◆ Increased strength of solder alloys
 - Finer microstructure
 - Less prone to grain coarsening
 - Restriction of dislocation movement and grain-boundary sliding
- ◆ Interconnection miniaturization
 - Very fine pitch applications
 - Increase fine pitch interconnection reliability

Environmental regulations require that solder alloys for electronic components and printed wiring board interconnections be lead free. Lead-free solder alloys such as Sn/Ag/Cu have become common. However, they generally have liquidus points of 220°C or higher, compared to the 183°C melting point of eutectic tin lead solder. The high melting point alloys require higher processing temperatures, with reflow process temperatures typically above 240–260°C.

These higher reflow temperatures may create greater residual stresses in board assemblies, which potentially reduce reliability. Components may be limited to those passing high-temperature qualifications. Higher temperatures sometimes require major changes in both manufacturing equipment and processes.

Many materials, including pure metals, exhibit a change in properties as their particle sizes approach nanoscale dimensions. The increase in the surface area-to-volume ratio, which occurs naturally as particle sizes shrink, necessarily increases the relative proportion of higher energy surface atoms. The effect may include a change in reactivity, such as in sinterability, the agglomeration of metal particles by heating. It may also appear as a change in electromagnetic properties, altering electronic or optical properties.

The particle size where these changes occur – the “tipping point” – depends on both the individual element or compound and its environment. Property changes normally require particle diameters to be somewhere below 100 nm. The tipping point shows as an abrupt shift in the slope of the measured curve. Figure 2.1 illustrates a tipping point in sinterability temperature as a function of the particle size.

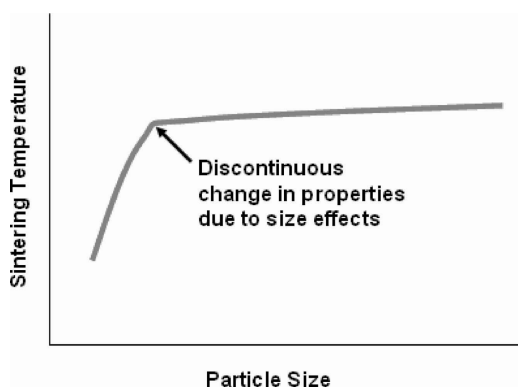


Fig. 2.1. Tipping point example

Solder materials containing nano-sized metals exploit the high surface area and high surface energy of nano-sized particles to lower the apparent melting point below the conventional melting point. Pure metals, such as Sn, Pb, and Cu, are known to show significant melting temperature depression, with the amount of temperature depression increasing as the particle size decreases. Thus the melting points of tin, silver and copper, the ingredients of lead-free solder, can all be depressed below 200°C, well below the eutectic melting point of 217°C.

Major challenges remain in developing lower temperature lead-free solders. The sub-20 nm particles must be uniform in size, well dispersed, and oxide free. However, researchers continue to show progress toward low melting point nanoparticle solder paste.

Tin (Sn) and its alloys are easily oxidized due to their low chemical potential. For nano-sized tin and its alloys, oxidation happens more easily due to the higher surface area-to-volume ratio of nanoparticles. The presence of oxides of the nanoparticles causes poor wetting and interconnection formation. Therefore, capping each nanoparticle to prevent oxidation is critical. The capping agents can cover the particle surfaces to serve as an effective barrier against the penetration of oxygen.

Jiang et al. [62] from Georgia Tech synthesized different sized 96.5Sn3.0Ag0.5Cu alloy nanoparticles by chemically reducing the precursors such as Tin (II) 2-ethylhexanoate, silver nitrate, copper nitrate. Effective capping capability can reduce or eliminate agglomeration of nanoparticles as well as protecting them from oxidation. It was found that some strong coordination agent could be an effective capping agent in forming crystalline SnAg alloy nanoparticles as shown in Fig. 2.2a, b, and c. When the SnAg alloy nanoparticles were formed, they were instantly coordinated through the pair of chelating nitrogen donor sites adjoining the two heterocyclic aromatic rings. The HRTEM characterizations (Fig. 2.2 c) showed that the particles were covered by capping agents which could provide an effective barrier against the penetration of atmospheric oxygen to the nanoparticles. At the same time, when using NaBH_4 as a reducing agent, hydrogen generated during a reduction reaction was found to be helpful in the creation of inert environments.

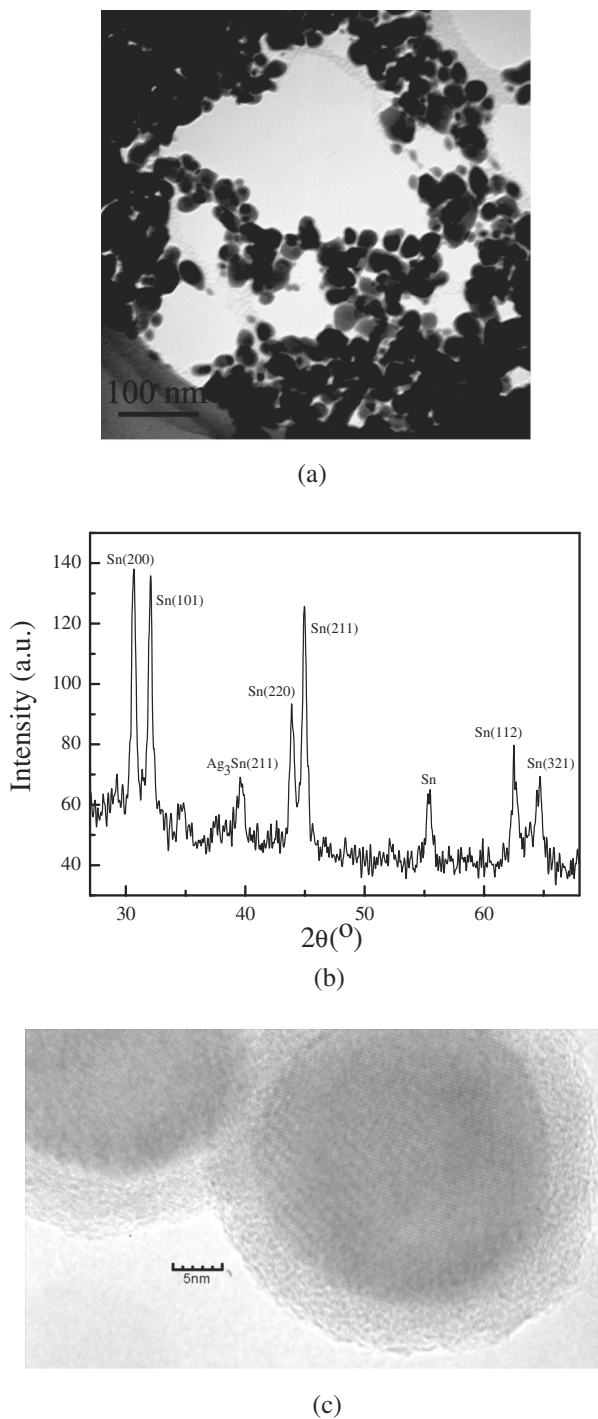


Fig. 2.2. TEM (a), XRD (b), and HRTEM (c) images of synthesized SnAg alloy nanoparticles

Then the author studied the melting behavior of the synthesized SnAg alloy nanoparticles by differential scanning calorimeter (DSC). Both the particle size-dependent melting point depression and the latent heat of fusion have been observed (Fig. 2.3). As can be seen from Fig. 2.3, as much as 25°C decreasing of melting point as the SnAg particle size was reduced to about 5 nm. It has already been found that surface melting of small particles occurs in a continuous manner over a broad temperature range, whereas the homogeneous melting of the solid core occurs abruptly at the critical temperature T_m [63, 64]. For smaller size metal nanoparticles, the surface melting is strongly enhanced by curvature effects. Therefore, both the melting point and the latent heat of fusion will decrease with the particle size.

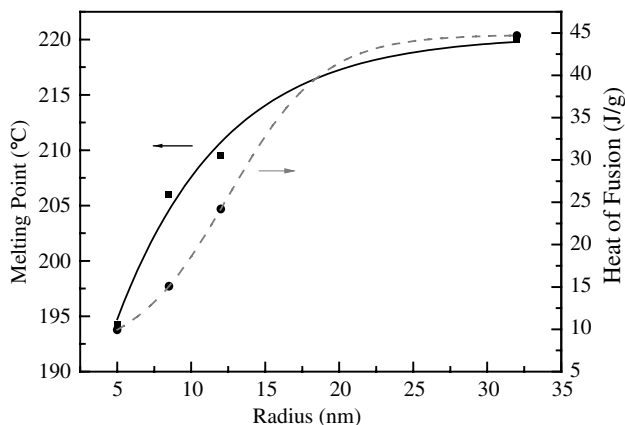


Fig. 2.3. Size-dependent melting of SnAg alloy nanoparticles by DSC

Although the nano alloys melt at a lower temperature, their wettability would be poorer than that of eutectic SnPb solders due to their intrinsically higher surface tension. Besides the intrinsic behavior of the nano alloys, the melting or sintering behavior of the nano alloy particles surrounded by liquids such as flux vehicles has not been investigated. Since all the theoretical approaches for the melting behavior of fine particles assume that the particles are placed in a free space, its behavior surrounded by the flux vehicle will be very interesting from a practical point of view.

To improve the wetting properties on the cleaned copper surface, the authors [62] formulated a nano solder paste by dispersing the SnAg alloy nanoparticles into a low viscosity acidic type flux. The synthesized particles were surface coated by capping agents to prevent oxidation. During the reflow process, the capping agents need to be debonded from the parti-

cle surfaces. Otherwise, they will hinder the wetting of particles on substrates. The desorption of these capping agents depends upon their affinity to the nanoparticle surfaces and their intrinsic thermal stability. Then the nano solder pastes were placed on top of the cleaned copper foil surface and then reflowed at 230°C in an oven with an air atmosphere for 5 min. A cross-sectional image of the sample after the reflow process was shown in Fig. 2.4. It was observed that the SnAg alloy nanoparticles with an average particle size of 64 nm completely melted and wetted on the cleaned copper foil surface. The energy dispersive spectroscopy (EDS) results revealed the formation of the intermetallic compounds (IMC) (Cu_6Sn_5), which showed scallop-like morphologies in Fig. 2.4. The thickness of the IMC was approximately 4.0 μm .

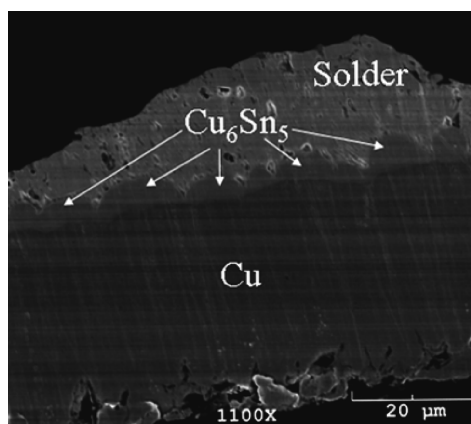


Fig. 2.4. A cross-sectional SEM image of a solder interface formed using the SnAg alloy nanoparticles (with an average particle size of 64 nm) on a cleaned copper foil surface after the reflow process

Guan et al. [65] successfully synthesized nanoparticles of Sn–4.0Ag–0.5Cu and Sn–0.4Co–0.7Cu (wt% composition) lead-free solder alloys using a top-down approach – spark erosion, also known as Consumable electrode Direct Current Arc (CDCA) or arc-discharge which has some advantages such as room temperature process, suitable for high volume production, and versatile. The manufacturing set-up, schematically shown in Fig. 2.5, shows the cathode (1), the anode (2) which are connected to a high current and low voltage power source, the bulk alloy electrodes (3 and 4), the arc discharge taking place between the electrodes (5), and the dielectric coolant (6). The nanoparticles are fabricated when the two electrodes come close enough to each other, so that a stable arc is formed. Different dielectric coolants such as liquid paraffin, glycerine, and

triethanolamine were used. Both glycerine and triethanolamine offered better oxidation protection compared to the liquid paraffin. However, due to the high viscosity of these two coolants, it became very difficult to extract the synthesized nanoparticles from the coolant. The synthesized nanoparticles were spherical in shape and with a size between 20 and 80 nm. High-resolution transmission electron microscopy (HRTEM) showed that the oxide layer thickness on the nanoparticles was about 2.5 nm. The melting point difference obtained by DSC (differential scanning calorimetry) for Sn–4.0Ag–0.5Cu and Sn–0.4Co–0.7Cu lead-free solders is between 1.1–7.8°C and 0.24–2.4°C, respectively, depending on the definition of the melting point determination by DSC.

Zhang et al. have showed that it is possible to control the particle size by changing the ultrasonic power. They have fabricated nanoparticles of Sn, Bi, and Sn–Bi by using ultrasonic vibration with a power of 900 W/cm² [66–68].

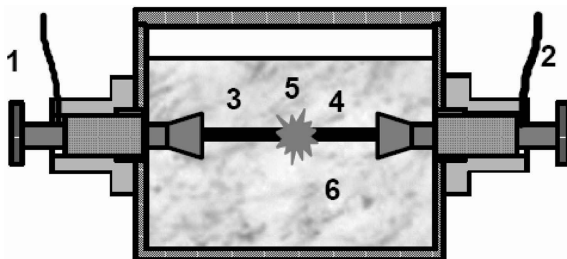


Fig. 2.5. A schematic drawing of an arc-discharge set-up for manufacturing nano solder particles

Recently there has been great research efforts to understand the effects of incorporating nanoparticles and nanotubes into the solders to the various properties of the bulk solder and also the intermetallic formation between the solder and the substrate pad finish.

Kumar et al. [69] studied the influence of nanopowders such as Ni, Cu, and Mo on the phase formation, microstructural characteristics, and mechanical behavior of conventional solder alloys (63Sn/37Pb and Sn/3.8Ag/0.7Cu). The composite solders were prepared by mechanical mixing of nickel (Ni), copper (Cu), and molybdenum (Mo) nano powders with solder alloys followed by cold compaction and sintering. It was observed that the intermetallics are uniformly distributed for the composite solders. The grain refinement of the composite solder occurs with addition of the nano sized metallic powders. The hardness of SnPb and SnAgCu composite solder increases with the increase in weight percentage of

nanopowders (Cu, Ni, and Mo). The addition of Mo to the SnPb and SnAgCu resulted in higher hardness values compared to that of adding Ni and Cu to the solders. The grain refinement and grain-boundary strengthening due to the nanopowders reinforcements are responsible for the improved deformation behavior of the composite solders.

Kumar et al. [70] investigated Sn/Ag/Cu (SAC) solders reinforced with SWCNTs, nano-nickel, and nano-Mo of varying weight percentages using a powder metallurgy method. The nanotubes were found to be homogeneously distributed at the edges of the grain boundaries of the Ag_3Sn intermetallic that are distributed evenly in the β -Sn solder matrix. Microstructure analysis revealed that the nano Ni and nano Mo particles were transformed to Ni_3Sn_4 and Mo–Sn intermetallic compounds during processing and distributed uniformly throughout the β -Sn solder matrix. When compared to the SAC solder without any reinforcement, composite solders exhibit enhanced hardness, enhanced yield strength, and enhanced ultimate tensile strength. However, the elongation to failure of the composite specimens considerably decreased. The increase in the strength of the nanocomposite solder specimens with respect to the wt% of SWCNT addition can be attributed to the critical reduction in the grain size. The enhanced mechanical properties also can be attributed to the effective load-transfer between the solder matrix and the nanotubes. The effect of brittle reinforcement content on the overall strength and ductility of the composite solder can be explained by the strengthening mechanisms such as stress gathering capability of the reinforcing particles, thermally induced matrix work hardening, a increase in dislocation density, and reduction of sub-grain size.

Qi et al. [71] investigated the effects of Ni nanoparticles addition on shear property and microstructure of Sn–3.5Ag lead-free solder joint. The nickel nanocomposite Sn–3.5Ag solder was prepared by adding dispersant to the dry nanoparticles and mechanically stirred Ni nanoparticles into the Sn–3.5Ag lead-free solder paste. The shear force of the Sn–3.5Ag solder, 0.5 and 1.0wt% nickel nanocomposite solder, was tested, respectively, at reflow 120 and 240s. The result showed that adding nickel nanoparticles could improve the shear performance of the soldered joint; the shear force of the soldered joint was highest when adding 0.5wt% Ni nanoparticles at reflow 240s. The SEM observations showed that the hexagonal Cu_6Sn_5 IMC (intermetallic compound) in the inside solder is disappears gradually and the morphsa of the IMC that on the interface of the solder joint becomes planar after adding Ni nanoparticles into solder.

To study the effect of nanoparticles on the growth of intermetallic compounds during reflow processes and thermal aging and on the drop-test performance, Amagai Masazumi [72] evaluated Co, Ni, Pt, Al, P, Cu, Zn, Ge, Ag, In, Sb, or Au inclusions in Sn–Ag-based lead-free solders. Also,

these nanoparticles were studied if they can reduce the frequency of occurrence of intermetallic compound fractures in high-impact pull tests. It was found that Co, Ni, and Pt were much more effective for depressing the growth of intermetallic compounds and enhancing drop-test performance than Cu, Ag, Au, Zn, Al, In, P, Ge, and Sb.

2.4 Carbon Nanotubes (CNTs)

Since the discovery in 1991, carbon nanotubes (CNTs) have developed into a distinct branch of nano-technology, nano-material, and nano-mechanical engineering with numerous unique applications. Carbon nanotubes (CNTs) are well-ordered, all-carbon hollow graphitic nano-materials with a high aspect ratio, lengths from several hundred nanometers to several micrometers with a diameter of 0.4–2 nm for single-walled (SWNT) and 2–100 nm for coaxial multiple-walled (MWNT) carbon nanotubes.

There are mainly two types of CNT, including single-walled CNTs (SWCNT) which consist of just one layer of graphite, and multi-wall CNTs (MWCNTs) which consist of two or more concentric shells of carbon and a hollow inner capillary. The separation between the adjacent shells in MWCNTs is about 0.34 nm.

In general, CNTs can be grown by arc-discharge, laser ablation, and chemical vapor deposition (CVD) methods (Table 2.1). However, for device applications, growth of CNTs by CVD methods is particularly attractive, due to features such as selective spatial growth, large area deposition capabilities, and aligned CNT growth.

Extensive experimental and theoretical studies have shown that CNT possess extraordinary electrical, mechanical, thermal, and chemical properties with a wide range of potential applications.

Table 2.1. Summary of CNT laboratory synthesis technique

	Arc discharge	Laser ablation	CVD
Carbon source	Graphite	Graphite	Hydrocarbon, CO
Energy source	Electricity	Laser	Plasma, furnace
Growth temp	2,500–3000°C	1,200°C	600–1100°C
Yield	30wt%	Up to 70wt%	20–100wt%
Scalability	Non-scalable	Non-scalable	Scalable
Advantages	-Few or no structural defects	-Diameter control -Few defects	-Relatively low temp -Long length Diameter control
Limitations	-High temp -Short tubes	-Costly -High power -Expensive laser	-High defects -Low crystallinity

As originally proposed, Moore's law states that the number of transistors in semiconductor devices or integrated circuits (ICs) doubles approximately every 18 months [73]. One of the historical consequences of increasing the number of devices on a chip and thus microprocessor performance is an associated increase in power consumption. Heat dissipation challenges create opportunities for fundamental research in materials and thermal management strategies. Specifically, it has been suggested that future cooling approaches may be based on micro- and nanotechnologies. For thermal management applications, the distinctive properties of one-dimensional structures and materials have gained much attention. Among such materials, carbon nanotubes (CNTs), due to their unique thermal properties, give rise to new opportunities in thermal management of microelectronic devices and ICs. Also, the extraordinary electrical and mechanical properties of CNTs make them a promising candidate for electrical interconnects [74, 75].

2.4.1 Carbon Nanotubes for Electrical Interconnect Applications

2.4.1.1 Electrical Properties of Carbon Nanotubes

Previous studies have demonstrated that a carbon nanotube behaves like a quantum wire due to geometrical confinement of the tube circumference [76]. The conductance of a multi-walled nanotube (MWNT) or a single-walled nanotube (SWNT) is determined by two factors: the conducting channels per shell and the number of shells. A SWNT consists of one shell. A SWNT rope or MWNT can be viewed as a parallel assembly of single SWNTs. Due to the structural imperfection of grown CNTs, the conductance for a SWNT, a SWNT rope, or MWNT can be written as

$$G = G_0 M = (2e^2 / h) M T \quad (2.1)$$

where M is an apparent number of conducting channels and T is the transmission probability for an electron through the contacts and the tube. Ideally, T is unity and $M = 2$ for a perfect ballistic SWNT less than 1 μm long. In actual operation, T may be significantly lower than 1 due to electron–electron coupling, intertube coupling effects, scattering from defects and impurities, structural distortions, and coupling with substrates or contact pads. Therefore, the experimentally measured conductance is much lower than the quantized value. Therefore, the high electrical resistance of a single nanotube necessitates the use of nanotube bundles aligned in parallel.

2.4.1.2 Carbon Nanotubes as Interconnects

There are two types of interconnects employed in microelectronic devices: horizontal and vertical. Horizontal interconnects link transistors in different locations on an integrated circuit; many layers of these horizontal interconnects (up to 12) can exist on a state-of-the-art circuit [77]. Each layer is then separated by an interlayer dielectric, generally porous SiO_2 or SiO_2 doped with C or F to lower its dielectric constant [78]. These materials are rather weak mechanically and are thermally unstable above $\sim 450^\circ\text{C}$. As dimensions decrease for on-chip interconnects, the current density carried by each interconnect increases. The International Technology Roadmap for Semiconductors (ITRS) predicts that in 2010 the current density will reach $5 \times 10^6 \text{ A/cm}^2$, a value which can only be supported by CNTs, since they are capable of a current density of $\sim 10^9 \text{ A/cm}^2$ [79].

Vertical interconnects pass through holes (vias) in the dielectrics to connect horizontal interconnects to the source, drain, or gate metallization of transistors. In existing microelectronic technology, the vias are fabricated from copper. Via regions are the most common source of failures in interconnect structures due to the high current densities and heterogeneous current distributions that cause electron-induced material transport (electromigration) [80]. Carbon nanotubes are expected to offer a substantially higher resistance to electromigration than do copper lines. Thus, CNT connections between metallization layers may solve the problems of electromigration and heat removal. Researchers from Fujitsu and Infineon have investigated this area extensively [81–83]. In one approach, a hole is etched in the interlayer dielectric, and catalyst is deposited into the bottom of the hole; excess catalyst is removed from the top of the hole. Alternatively, a catalyst layer is deposited under the interlayer dielectric and is exposed by etching a hole in the dielectric. In both approaches, CNTs are then grown within the hole by CVD or by plasma-enhanced CVD (PECVD).

When interconnects and vias are further reduced in size to meet requirements for future ICs, CNT vias will offer still more advantages. Vias consisting of only one MWNT are conceivable, since multi-walled nanotubes can be produced with diameters from 5 to 100 nm; indeed, Infineon has demonstrated such a process [81].

To take full advantage of CNT ballistic conductivity, one must open the CNT ends after growth [84] to permit better wetting and contact by Sn/Pb, etc. CNT flip chip electrical interconnection is also under study [85–88], with micrometer m-scale CNT clusters successfully developed as flip chip “nano-bumps” [89]. Au and Ag incorporation into CNTs has also been studied for electrical contacts with minimal galvanic corrosion [90]. Metal and carbon loaded polymers have long been used for high-frequency conductors in electromagnetic shielding, and both carbon fibers and multi-walled CNTs have been studied in polymer matrices for the purpose [91, 92]. CNT replacement of ICA metal filler, however, does not even match the electrical conductivity of standard materials.

2.4.1.3 Carbon Nanotubes for Thermal Management

Several investigations have indicated that CNTs have unusually high thermal conductivity in the axial direction. For example, molecular dynamics simulations of a SWNT by Berber et al. indicated that the thermal conductivity of a SWCNT can be as high as 6,600 W/mK at room temperature [93]. Dai et al. presented a method for extracting the thermal conductivity of an individual SWNT from high bias electrical measurements in the temperature range from 300 to 800K by reverse fitting the data to an existing electrothermal transport model [94]. The thermal conductivity measured was nearly 3,500 W/mK at room temperature for a SWNT of length 2.6 μm and diameter 1.7 nm. Kim et al. developed a microfabricated suspended device hybridized with MWNTs ($\sim 1 \mu\text{m}$) to allow the study of thermal transport where no substrate contact was involved [95]. The thermal conductivity and thermoelectric power of a single carbon nanotube were measured, and the observed thermal conductivity is $>3,000 \text{ W/mK}$ at room temperature.

Hone et al. measured the thermal conductivity of aligned and unaligned SWNTs from 10 to 400K [96]. Thermal conductivity increased smoothly with increasing temperatures for both aligned and unaligned SWNTs. At room temperature, the thermal conductivity of aligned SWNTs was greater than 200 W/mK, compared to $\sim 30 \text{ W/mK}$ of unaligned ones; above 300K, the thermal conductivity increased and then leveled off near 400K. Yi et al. measured the thermal conductivity of millimeter-long aligned MWNTs [97]. The thermal conductivity was low, only $\sim 25 \text{ W/mK}$, at room temperature, due to a large number of CNT defects. However, thermal conduc-

tivity could reach $\sim 2,000$ W/mK if the aligned MWNTs were annealed at $3,000^{\circ}\text{C}$ to remove the defects. Yang et al. investigated the thermal conductivity of MWNT films prepared by microwave CVD using a pulsed photothermal reflectance technique [98]. The average thermal conductivity of carbon nanotube films, with the film thickness from 10 to $50\text{ }\mu\text{m}$, was ~ 15 W/mK at room temperature and independent of tube length. However, by taking into account a small volume filling fraction of CNTs, the effective nanotube thermal conductivity can reach 200 W/mK.

Aligned CNTs have been grown directly on silicon surfaces for thermal management. Xu et al. grew aligned CNTs on silicon wafers using plasma-enhanced CVD [99]. The thermal testing performed was based on a one-dimensional reference bar method in high vacuum with radiation shielding, and temperature measurements were carried out with an infrared camera. Dry CNT arrays have a minimum thermal interface resistance of $19.8\text{ mm}^2\text{K/W}$, while CNT arrays with a phase change material (PCM) produced a minimum resistance of $5.2\text{ mm}^2\text{K/W}$. Xu et al. used a photothermal metrology to evaluate the thermal conductivity of aligned CNT arrays grown on silicon substrates by plasma-enhanced CVD [100]. The effective thermal resistance was $12 - 16\text{ mm}^2\text{K/W}$, which is comparable to the resistance of commercially available thermal grease. K. Zhang et al. [101] fabricated aligned carbon nanotube (CNT) arrays from a multilayer catalyst configuration by microwave plasma-enhanced chemical vapor deposition (PECVD). One of the potential applications of CNT is thermal interface materials (TIMs). TIM is used to fill the gaps between thermal transfer surfaces, such as between microprocessors and heatsinks, in order to increase thermal transfer efficiency. These gaps are normally filled with air which is a very poor conductor. Figure 2.6 shows two typical packaging architectures used in electronics cooling [102]. For example, TIM1 between the chip and the heat spreader and TIM2 between the heat spreader and the heat sink have been introduced to fill the gap between the asperities to minimize the contact thermal resistance. The effects of the thickness and annealing of the aluminum layer on the CNT synthesis and thermal performance were investigated. It was demonstrated that the CNT-thermal interface material (CNT-TIM) reduced the thermal interfacial resistance significantly compared with state-of-the-art commercial TIM. The total thermal resistance of the CNT-TIM was only $7\text{ mm}^2\text{KW}^{-1}$ and was about 10% of that of commercial silver epoxy TIM. The light performance of high-brightness light-emitting diode (HB-LED) packages using the aligned CNT-TIM was tested. The results indicated that the light output power was greatly improved with the use of the CNT-TIM. The usage of the CNT-TIM can be also extended to other microelectronics thermal management applications.

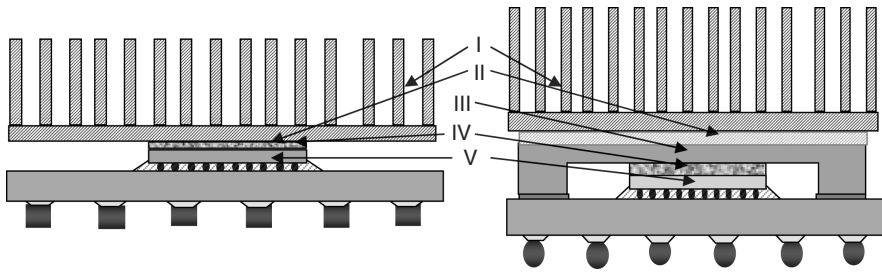


Fig. 2.6. Schematic illustration of the two thermal architectures. (a) Architecture I, typically used in laptop applications. (b) Architecture II, typically used in desktop and server applications. I, – heat sink; II, – TIM2; III, – IHS; IV, – TIM1; V, – die; VI, – underfill; VII, – package substrate [102]

The high CNT thermal conductivity is used directly for conductive cooling of chips and indirectly in convective cooling [103]. For conductive systems, CNT alignment is the problem, since the thermal conductivities of random arrays show no advantages over conventional materials. Composites filled with CNTs have also been studied for thermal interface materials, e.g., CNT/carbon black mixtures in epoxy resin. The use of a liquid crystal resin matrix can impose structural order on the CNT alignment to yield a seven-fold improvement in thermal conductivity [104]. Recently, electrospun polymer fibers filled with CNTs, or with SiC or metallic nanoparticles, have shown advances in both mechanical and thermal properties [105].

Micron-scale clusters of vertically grown nanotubes [106, 107] define microchannels for convective cooling coolant flow, similarly to the metal or silicon structures they aim to replace, with similar thermal performances. The problem is that the flowing coolant is only in contact with the outermost CNTs of the clusters, and the internal CNTs are not even in good contact with each other. The system has been modeled, and the solution is clearly to spread the CNTs apart by an optimal separation to permit coolant contact with each one. The problem then is whether individual CNTs can withstand the coolant flow pressure without detaching from the substrate.

2.4.1.4 Integration of Carbon Nanotubes into Microsystems

For electronic device applications, chemical vapor deposition (CVD) methods are particularly attractive. However, the CVD technique suffers from several drawbacks. One of the main challenges for applying CNTs to circuitry is the high growth temperature ($>600^{\circ}\text{C}$). Such temperatures are incompatible with microelectronic processes, which are typically performed below $400\text{--}500^{\circ}\text{C}$ in backend-of-line sequences. Another issue is the poor adhesion between CNTs and the substrates, which will result in long-term reliability issues and high contact resistance. At the device level, CNTs must be integrated and interconnected with metal electrodes to allow signal input and output. Typical approaches for CNT growth on such substrates involve the deposition of catalysts such as Fe or Ni on metal layers such as Ti or Ti/Au. Unfortunately, results indicate that electrical contact is not necessarily improved, suggesting that attachment of CNTs onto the electrodes produces poor mechanical and electrical properties yielding high contact resistance. On the other hand, to meet manufacturing requirements and throughput for IC applications, a large number of CNTs must be positioned simultaneously rather than aligning CNTs one by one.

To overcome the above disadvantages, Zhu et al. at Georgia Tech proposed a methodology termed “CNT transfer technology,” which is enabled by open-ended CNT structures [84]. This technique is similar to flip chip technology as illustrated schematically in Fig. 2.7.

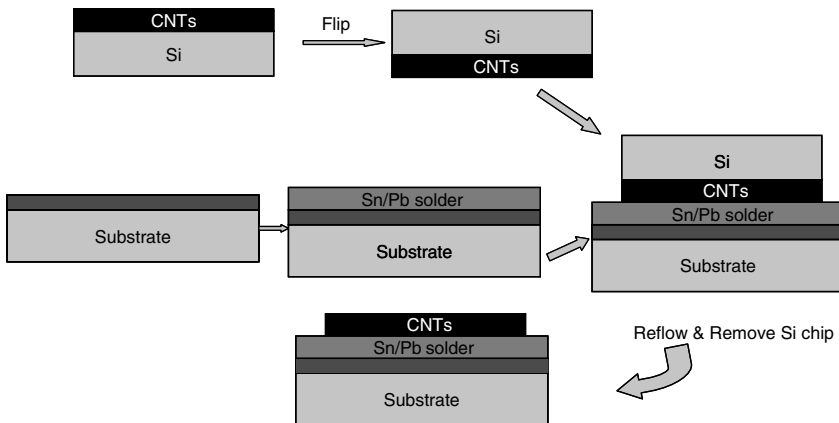


Fig. 2.7. Schematic diagram of “CNT transfer technology” [84]

The eutectic tin–lead paste is stencil printed on a copper substrate. After reflow, the tin–lead solder is polished to 30 μm thick. The silicon substrates with CNTs are then flipped and aligned to the corresponding copper substrates and reflowed in a reflow oven to simultaneously form electrical and mechanical connections. This process is straightforward to implement and offers a strategy for both assembling CNT devices and scaling up a variety of devices fabricated using nanotubes (e.g., flat panel displays). This process offers an approach to overcome the serious obstacles of integration of CNTs into integrated circuits and microelectronic device packages by offering low processing temperatures and improved adhesion of CNTs to substrates. Figure 2.8 shows the demarcation between the broken CNTs and the intact and connected ones. When pulled from the substrate, the CNTs break along the axis rather than at the CNT–solder interface. The excellent mechanical bonding strength of CNTs on the substrate anchors the CNTs and thereby improves the CNT/substrate interfacial properties.

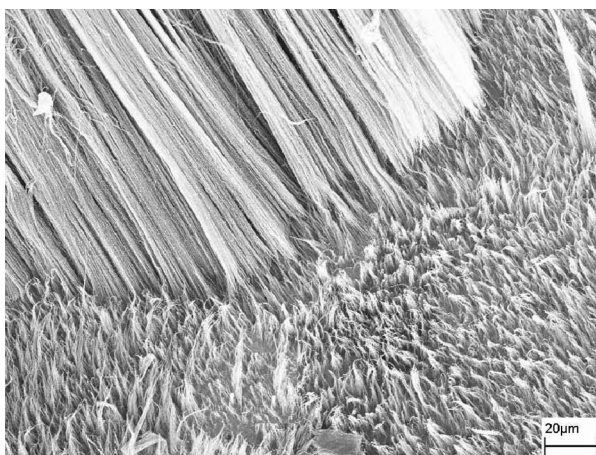


Fig. 2.8. SEM of the copper substrates on which the CNTs were assembled after some CNTs were pulled from the surface by tweezers; this figure demonstrates the excellent mechanical bond strength of CNTs transferred to the copper substrate by the solder reflow process [84]

Recently, Lin et al. from Georgia Tech proposed another new transfer technology for aligned CNT, named “chemical transfer” (Fig. 2.9). Chemical transfer is a two-step assembly process, (1) well-aligned CNTs are in situ functionalized (f-ACNTs) during the CVD growth; (2) f-ACNTs are then anchored onto the gold-coated substrate by forming covalent bonding between the f-ACNTs and the self-assembled monolayer of conjugated thiol molecules on the gold surface. The in situ functionalization process

allows for precise length control of ACNT assembly without randomly damaging the CNT structures and, equally importantly, renders the ACNT surface, especially the opened ends, chemically reactive to certain functional groups [108]. In their publication, a chemically transferred ACNT film on the gold surface with self-assembled monolayer of conjugated thiol molecules was successfully demonstrated (Fig. 2.10).

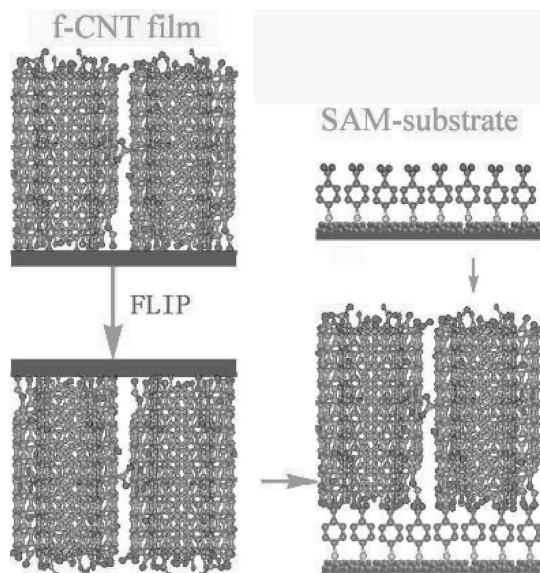


Fig. 2.9. Schematic illustration of the chemical transfer process [108]

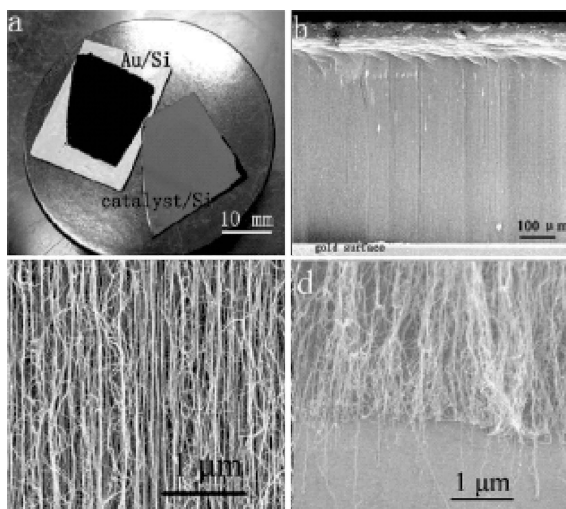


Fig. 2.10. Chemically transferred f-ACNT film on the gold surface: (a) photograph; (b) the side view SEM image (by 0.5 N/cm² of compressive force during transfer); (c) further enlargement of the CNT alignment after chemical transfer; and (d) the anchored f-ACNT/gold interface after part of the transferred ACNTs was removed [108]

The chemically transferred f-ACNT showed a linear current–voltage (I – V) curve which suggested an Ohmic contact (Fig. 2.11). The resistivity of the individual ACNT was demonstrated to be in the order of $10^{-4} \Omega\text{-cm}$. The authors attributed the Ohmic contact and low resistance to two factors, conjugated SAM-assisted bonding and relatively low defect density. This process offers the opportunity of using ACNT in broader applications such as electrical interconnect, thermal transport, electrodes for sensors.

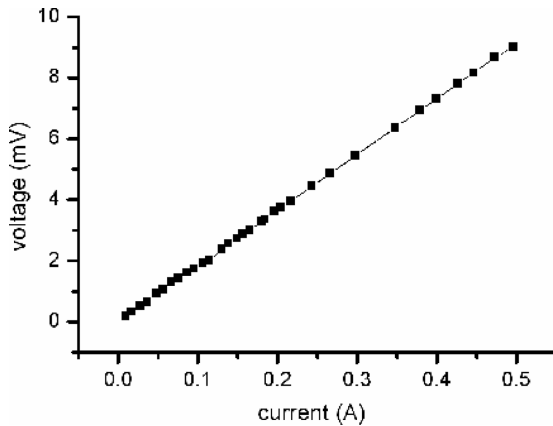


Fig. 2.11. The room temperature I – V curve of the f-ACNT/gold interconnect via the chemical transfer [108]

2.4.1.5 Summary and Future Needs

Scaling of microelectronic devices has led to an interest in utilizing carbon nanotubes for electrical interconnects and thermal management approaches. Carbon nanotubes are also promising for vertical interconnects (for on-chip or packaging levels) and heat removal for microelectronics packaging. CNTs may be able to meet some of the ITRS projections for device interconnects and thermal requirements. However, a number of materials and CNT process integration issues need to be addressed before a CNT technology platform can be developed, including growth of structurally perfect carbon nanotubes, chirality control of carbon nanotubes, and positioning of carbon nanotubes in predefined locations simultaneously. The barriers to CNT implementation in the packaging of microelectronic devices and ICs offer numerous opportunities for new developments and

approaches. Clearly, more effort is required in order to take CNT technologies from the research laboratory to high-volume production.

2.5 Nanocomposites

2.5.1 Recent Advances in Nanocomposites

Nanocomposites are materials that are created by introducing nanoparticulates (often referred to as filler) into a macroscopic sample material (often referred to as the matrix). This is part of the growing field of nanotechnology. After adding nanoparticulates to the matrix material, the resulting nanocomposite may exhibit drastically enhanced properties. For example, adding carbon nanotubes tends to drastically improve the electrical and thermal conductivity. Other kinds of nanoparticulates may result in enhanced optical properties, dielectric properties, or mechanical properties such as stiffness and strength. In general, the nanosubstance is dispersed into the matrix during processing. The percentage by weight (called mass fraction) of the nanoparticulates introduced can remain very low (on the order of 0.5–5%) due to the incredibly low filler percolation threshold, especially for the most commonly used non-spherical, high aspect ratio fillers (e.g., nanometer thin platelets, such as clays, or nanometer diameter cylinders, such as carbon nanotubes).

The internal surfaces are critical in determining the properties of nano-filled materials. Nanoparticles have high surface area-to-volume ratio; particularly when the size decreases below 100 nm. This high surface area-to-volume ratio means that for the same particle loading, nanocomposites will have a much greater interfacial area than microcomposites. This interfacial area leads to a significant volume fraction of polymer surrounding the particle that is affected by the particle surface and has properties different from the bulk polymer (interaction zone) [109]. Since this interaction zone is much more extensive for nanocomposites than for microcomposites, it can have significant impact on properties (shown in Fig. 2.12) [110, 111].

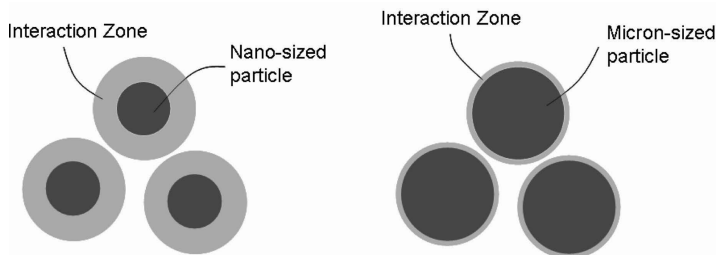


Fig. 2.12. A schematic comparison of particle and matrix interaction in nanocomposites and microcomposites

For example, depending upon the strength of the interaction between polymer and particle, this region can have a higher or lower mobility than the bulk material and result in an increase or decrease in glass transition temperature [112]. It has also been suggested that free volume in such interaction zones is altered by the introduction of nano-fillers. Since these interaction zones are likely to overlap at relatively low-volume fractions in nanocomposites, a small amount of nano-filler has been found to impact the electrical behavior [113, 114]. Some authors have emphasized that the interaction zone around the particles is a “quasi-conductive” region which partially overlaps in the nanocomposites [114]. These overlapped interface regions thus may allow charge dissipation, which, in turn, could improve the dielectric breakdown strength and voltage endurance characteristics. Introduction of a second phase can also influence the breakdown strength of the dielectrics via a scattering mechanism (i.e., an increase in path length of the carriers responsible for the breakdown processes) or, by changing the space-charge distribution [115]. It has been shown by some authors that when the size of the filler approaches the chain conformation length, they act “cooperatively” with the host structure either eliminating or suppressing Maxwell–Wagner polarization, which is well known in the case of conventionally filled materials [116]. Some recent results also suggest that it is the size of the filler that plays the most crucial role in terms of global properties (electrical, mechanical, and thermal), rather than the chemistry of the particles [117]. Finally, changes in morphology due to incorporating nanoparticles can influence the dielectric behavior of nanocomposites [118]. The large surface area can also lead to changes in the morphology of semicrystalline polymers as observed by several groups [118]. The breakdown strength of the intraspherulitic regions is higher than that of the interspherulitic regions and a change in the disorder within the spherulites or of the interspherulitic region can affect the breakdown strength. In addition, it is important to recognize that nanoparticle/fibrous loading confers significant property improvements with very

low loading levels, traditional microparticle additives requiring much higher loading levels to achieve similar performance. This in turn can result in significant weight reductions, which is important for various military and aerospace applications, for similar performance, greater strength for similar structural dimensions and, for barrier applications, increased barrier performance for similar material thickness.

Roy et al. [56] studied the effect of interactions between the nanoparticle surface and the matrix to the electrical properties of the nanocomposite. It was found that covalent bonding between the nanoparticles and the matrix (vinylsilane treated nanoparticles) increases the temperature at which the breakdown strength decreases. The increase in interfacial region in nanocomposites creates a zone of altered polymer properties which reduces the dielectric permittivity of nanocomposites. The highest voltage endurance occurs for composites with strong covalent bonding between the matrix and the filler.

Ramanathan et al. [119] described the use of SWNTs to create low-volume fraction polymer composites with dramatically improved mechanical, thermal, and electrical properties when compared with those of the neat polymer. Composites were created with unmodified and amide-functionalized the SWNTs (a-SWNT). The formation of amide groups on the surface of SWNTs provides free amine groups to interact with PMMA, and IR spectra indicated covalent bonding between a-SWNT and PMMA. For both SWNT/PMMA and a-SWNT/PMMA composites, thermal, mechanical, and electrical data showed significantly improved properties when compared with those of the neat polymer. The experimental results also demonstrated that the a-SWNT/PMMA composite properties are consistently improved when compared with those of the SWNT/PMMA composite. The increase in thermal degradation temperature, glass transition temperature (T_g), storage modulus, and electrical conductivity confirms better interaction between the functionalized SWNTs and the polymer. Functionalized SWNT resulted in a composite where relaxation mechanisms ($\tan \delta$) are shifted by 30°C from that of the matrix material, indicating extensive interphase regions and absence of PMMA with bulk properties. In contrast, the composite with unmodified nanotubes retained the dominant relaxation characteristics of the bulk PMMA with a broadening of the loss peak, indicating existence of discrete interphase regions near the nanotubes. The mechanical property data were compared with modeling predictions based on ideal dispersions of randomly oriented straight SWNTs in PMMA. The modulus properties for both composites significantly exceed the predicted upper bound. These results reinforce the existence of an extensive polymer interphase in both composites with altered properties. These results further demonstrate that the altered polymer near the nanotubes has increased modulus, consistent with the loss modulus

data indicating decreased mobility of the polymer in the interphase region. The consistent improvement in the properties of the a-SWNT composite when compared with those of the SWNT composite can be attributed to the increased extent of the interphase with altered properties and finer dispersion of nanotubes due to the functionalization.

The results here indicate promising potential for polymer nanocomposites with enhanced thermal, mechanical, and electrical properties. The demonstrated importance of the interphase region underscores the need for more detailed modeling and characterization to understand the changes in local polymer dynamics near nanoparticles and the percolation of these effects in distributed systems. The success of the functionalization to provide consistently improved properties in this work indicates the possibility to create designer nanocomposites with controlled interface chemistry and interphase zones and thus controlled load transfer and properties.

2.5.2 Areas of Application of Nanocomposites

The mechanical property improvements of nanocomposites have resulted in major interest in nanocomposite materials in numerous automotive and general/industrial applications. These include potential for utilization as mirror housings on various vehicle types, door handles, engine covers, and intake manifolds and timing belt covers. More general applications currently being considered include usage as impellers and blades for vacuum cleaners, power tool housings, mower hoods, and covers for portable electronic equipment such as mobile phones, pagers, etc.

The substantial gaseous barrier property improvement that can result from incorporation of relatively small quantities of nano-filler has resulted in considerable interest in nanoclay composites in food packaging applications, both flexible and rigid. The use of nanocomposite formulations would be expected to enhance considerably the shelf life of many types of food.

The ability of nanoclay incorporation to reduce solvent transmission through polymers such as polyamides has resulted in considerable interest in using these materials as both fuel tank and fuel line components for cars. Of further interest for this type of application, the reduced fuel transmission characteristics are accompanied by significant material cost reductions.

The presence of nano-filler incorporation has also been shown to have significant effects on the transparency and haze characteristics of films. In comparison to conventionally filled polymers, nanocomposite has shown to significantly enhance transparency and reduce haze. When employed to coat polymeric transparency materials, the nanocomposites can enhance both toughness and hardness of these materials without interfering with light transmission characteristics.

Kim et al. [120] investigated the moisture diffusion and barrier characteristics of epoxy-based nanocomposites containing organoclay. It was found that moisture diffusivity of nanocomposites decreased with increasing clay content. The moisture permeability showed a systematic decrease with increasing clay content. It was also observed that high aspect ratio nanoparticle showed the lowest moisture permeability because of the increased effective penetration path caused by the aspect ratio nanoparticles. Similar effects have been observed by van Es of DSM with polyamide based nanocomposites. In addition, van Es noted a significant effect of nanoclay aspect ratio on water diffusion characteristics in a polyimide nanocomposite. Specifically, increasing aspect ratio was found to diminish substantially the amount of water absorbed, thus indicating the beneficial effects likely from nanoparticle incorporation in comparison to conventional microparticle loading. Hydrophobic enhancement would clearly both improve nanocomposite properties and diminish the extent to which water would be transmitted through an underlying substrate. Thus applications in which contact with water or moist environments is likely could clearly benefit from materials incorporating nanoclay particles.

The ability of nanoclay incorporation to reduce the flammability of polymeric materials was a major theme of the paper presented by Gilman [121]. In his work Gilman demonstrated the extent to which flammability behavior could be restricted in polymers such as polypropylene with as little as 2% nanoclay loading. Although conventional microparticle filler incorporation, together with the use of flame retardant and intumescent agents would also minimize flammability behavior, this is usually accompanied by reductions in various other important properties. With the nanoclay approach, this is usually achieved while maintaining or enhancing other properties and characteristics.

2.6 Nano Interconnect

2.6.1 Carbon Nanotube Transistors

Semiconducting CNTs have been used to fabricate field-effect transistors (CNTFETs), which show promise due to their superior electrical characteristics over silicon-based MOSFETs. Since the electron mean-free path in SWCNTs can exceed 1 μm , long channel CNTFETs exhibit near-ballistic transport characteristics, resulting in high-speed devices. In fact, CNT devices are projected to be operational in the frequency range of hundreds of GHz. Recent works detailing the advantages and disadvantages of various forms of CNTFETs have also shown that the tunneling-based CNTFET offers better characteristics compared to other CNTFET structures. This device has been found to be superior in terms of subthreshold slope – a very important property for low-power applications.

Carbon nanotube field-effect transistors (CNTFETs) were fabricated with metal material (gold) and semiconductor material (bismuth telluride, Bi_2Te_3) as the source and drain materials [122]. Highly purified single-walled carbon nanotubes (CNTs) were used for the fabrication of CNTFETs. The single-walled carbon nanotubes were ultrasonically dispersed in toluene and dimethylformamide (DMF) with trifluoroacetic acid (TFA), as co-solvent. Dielectrophoresis (DEP) method was used to deposit, align, and assemble carbon nanotubes (CNTs) to bridge the gap between the source and the drain of CNTFETs to form the channel. The structure of CNTFET is similar to a conventional field-effect transistor with substrate acting as a back-side gate. Electron-beam evaporation was used to deposit gold and bismuth telluride thin films. Microfabrication techniques such as photolithography, e-beam lithography, and lift-off process were used to define and fabricate the source, drain, and gate of CNTFETs. The gap between the source and the drain varied from 800 nm to 3 μm . It was found that in the case of gold (Au) electrodes, the I - V curves of CNTFETs clearly show behavior of the CNT (metallic or semiconducting) aligned across the source and drain of CNTFETs, while in the case of bismuth telluride electrodes, the I - V curves are less dependent on the type of CNTs (metallic or semiconducting). The developed carbon nanotube field-effect transistors (CNTFETs) can be a good candidate for the application of nanoelectronics and integrated circuits with a high mobility and fast switching.

Srivastava et al. [123] evaluated CNT bundle interconnects against Cu interconnects from performance, power dissipation, and thermal management/reliability perspectives. The equivalent circuit parameters for a CNT

bundle interconnect were explicitly calculated and it was found that CNT bundles can significantly improve the performance of long global interconnects by as much as 80% with minimal additional power dissipation (for maximum metallic CNT density). Moreover, power-optimal repeater insertion methodology can be applied to CNT bundle interconnects (just as with Cu) to save power with a small delay penalty. Most importantly, it was shown that CNT bundle vias can greatly reduce interconnect temperature rise and thus, when integrated with Cu interconnects, tremendously improve Cu interconnect performance (about 30%) and lifetime (by at least two orders of magnitude) due to lower temperatures. The advantage of CNT bundle vias in controlling the back-end temperature, as shown in this work, will also have significant implications for emerging technologies such as three-dimensional ICs where thermal management is a big concern. Similarly, researchers at Rensselaer Polytechnic Institute, based on their latest results from advanced quantum mechanical computer modeling to run vast simulations on a high-powered supercomputer, concluded that the carbon nanotube bundles boasted a much smaller electrical resistance than the copper nanowires (<http://www.sciencedaily.com>). This lower resistance suggests carbon nanotube bundles would therefore be better suited for interconnect applications.

2.6.2 CNT Via

Some very interesting results have been achieved by Kawabata et al. [124] recently on integrating CNT in the via at a CNT growth temperature as low as 400°C. The fabrication processes are compatible with conventional LSI processes. Briefly, a substrate with a Cu interconnect covered by a dielectric layer was first prepared. The dielectric layer was SiOC with $k = 3.0$ or $k = 2.6$ (ultra-low K dielectric). Via holes with a diameter of 160 nm were made using conventional photolithography followed by dry etching. A TaN/Ta barrier layer and a TiN contact layer were deposited by physical vapor deposition (PVD). Size-controlled Co particles with a mean diameter of about 4 nm were then deposited using a nanoparticles deposition system. MWNTs were grown by thermal CVD with C_2H_2 diluted by argon as the source gas. The substrate temperature ranged from 365°C to 450°C. The substrate with MWNTs was then coated with spin-on glass (SOG) and planarized by chemical mechanical polishing (CMP). The CMP condition was similar to the one used for polishing a silicon dioxide layer. Finally, a Ti top contact layer, a Ta barrier layer and a Cu wire were connected to the CNT vias by PVD. Figure 2.13a shows a schematic of via stack structure and Fig. 2.13b shows a SEM image of a via with grown CNTs. The fabricated CNT via interconnect with a diameter of 160 nm was evaluated for

its robustness over a high density current. CNTs used for fabricating vias were grown at temperatures at 400°C. At such low temperatures, the ultra-low k dielectric layer ($k = 2.6$) used in the via structure was not damaged. Electrical measurement showed that the CNT via was able to sustain a current density as high as $5.0 \times 10^6 \text{ A/cm}^2$ at 105°C for 100 h without properties degradation. And we plan to measure the robustness more than higher current density. The authors are working on fabricating CNT vias at temperature lower than 400°C which will be helpful in realizing reliable CNT vias for future LSIs.

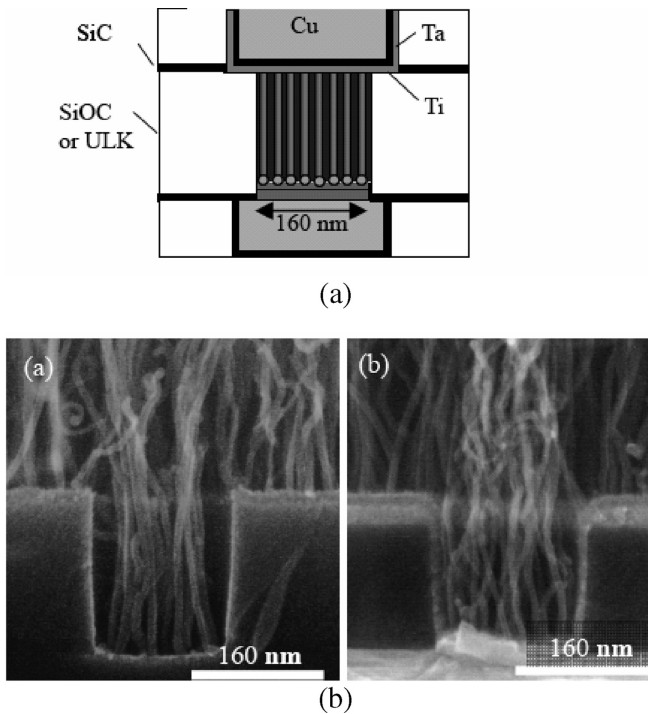


Fig. 2.13. (a) A schematic of via stack structure with CNTs and (b) SEM image of a via with CNTs which were grown at 450°C (*left*) and 400°C (*right*) [142]

2.6.3 CNT as Flip Chip Interconnect

Soga et al. [125] reported on CNT bumps for the flip chip interconnect instead of solder bumps. The CNT bumps were formed on the electrodes on a chip by the CNT pattern transfer process. To measure the resistance of CNT bumps, CNT bump contact chains were fabricated. It was found that

coating the CNT bumps with gold greatly improved the contact resistance of the bumps with the chip and the host substrate, resulting in a lower bump resistance of 2.3Ω which is still too high for any practical applications. It was also demonstrated that the CNT bumps were able to absorb a displacement between the chip and the substrate up to 10 – 20% of the CNT bump height. The resilience and flexibility of CNT bumps makes them very attractive for realizing thermal stress-free flip chip structure.

Iwai et al. [126] from Fujitsu also demonstrated the use of CNT bumps to provide both electrical and thermal conduction between a high power amplifier flip chip die and a AlN substrate. The CNT bundles were grown directly on the pre-defined areas on the AlN substrate. By using the CNT bumps, heat was more effectively removed from the die and the grounding impedance was reduced significantly and, as a result, high gain was achieved.

2.6.4 Nanoparticle Interlayer for Copper to Copper Bonding

Metallic nanoparticles of copper and gold are explored and evaluated for the nanostructured bonding layers between the copper surfaces [127]. High surface energy of the nanoparticle lowers the melting temperature of the material, and hence, enhances inter-diffusion kinetics that helps in faster bonding rate. In addition, high surface energy and high grain boundary-to-volume ratio endow the particles with elaborate mobility making the diffusion kinetic even faster. It was demonstrated that the nanoparticles formed on the copper surface could reduce the bonding temperatures.

2.6.5 Interconnection Using Inkjet Printing of Nano-ink

The use of nanoparticles of metals with high electric conductivity provides new prospects for direct printing of conductive patterns. The microfabrication of conductive tracks by photolithographic and electroless techniques are time consuming, expensive processes, and there is an industrial need for direct digital printing to simplify the processes and to reduce manufacturing costs [128, 129]. Furthermore, it is desirable to fabricate onto polymeric or similar temperature sensitive substrates by solution-based printing process. Metallic conducting tracks of low resistance must be achieved at temperatures sufficiently lower so as to be compatible with organic electronics on plastic substrates.

Direct metal printing needs to be processed with ink materials that can convert to a low-resistance conductor after solvent removal and heat treatment. Two approaches have been pursued to attain these goals. The first is to use solutions of metallorganic precursors where the molecular

nature of the compound allows low-temperature reduction to the metal [130–132]. A second route is the use of suspensions of metal particles of nano-size diameters whose small size endows a reduction in melting temperature that is significantly lower than that of the bulk material [128, 133, 134]. As an example, Fuller et al. [133] reported a method to additively build three-dimensional (3-D) microelectromechanical systems (MEMS) and electrical circuitry by ink-jet printing nanoparticle gold and silver colloids. Fabricating metallic structures from nanoparticles avoids the extreme processing conditions required for standard lithographic fabrication and molten metal droplet deposition. Nanoparticles typically measure 1–100 nm in diameter and can be sintered at plastic-compatible temperatures as low as 300°C to form material nearly indistinguishable from the bulk material. Multiple drops were deposited to leave a conductive line or surface (see Fig. 2.14). Multiple ink-jet print heads mounted to a computer-controlled 3-axis gantry deposit the 10% by weight metal colloid ink layer by layer onto a heated substrate to make two-dimensional (2-D) and three-dimensional structures. The author reported a high-Q resonant inductive coil, linear and rotary electrostatic-drive motors, and in-plane and vertical electrothermal actuators. The results suggested a route to fabricate a large-area MEMS system characterized by many layers, low cost, and data-driven fabrication for rapid turn-around time.

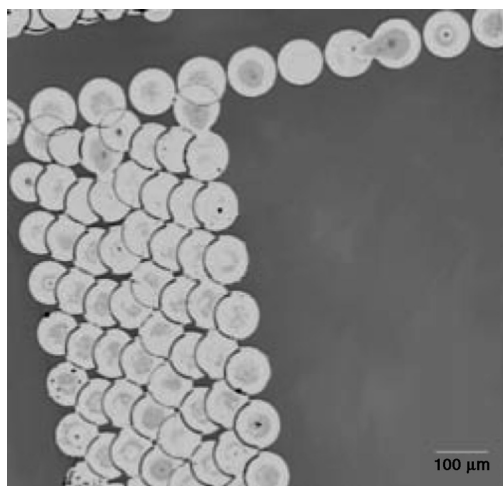


Fig. 2.14. Optical micrograph of an arrangement of sintered ink-jet printed-nanoparticle gold droplets on plastic polyimide film. Electrically conductive lines and three-dimensional structure are fabricated by printing multiple layers of droplets

Various types of printing wiring circuits are expected to become one of the key technologies for the advanced electronics packaging. The combination with metallic nanoparticles pastes can provide new tools for fine pitch and three-dimensional electronics circuits. Especially, with the combination of Ag nanoparticles pastes and ink-jet printing, one can obtain a lot of benefits as

- on-demand fabrication;
- environmental consciousness/economy;
- three-dimensional stacking;
- fine pitch lines and spaces;
- easy scale up of products;
- wide material selections and;
- small quantity but variety of products.

Kim et al. [135] demonstrated a direct metal printing of the Ag nanoparticles on plastic substrates. The granular Ag films become highly conductive, roughly $3.2 \mu\Omega \text{ cm}$, when heat treated even at 200°C . The Ag particles of smaller size (21 nm) are more reactive than the larger sized particles (47 nm).

The relatively high curing temperature limits the application of nanoparticle inks only to the applications of heat-resistant substrates. K. Suganuma et al. [136] have recently developed a new type of ink for wiring metallic Ag lines. The inks are Ag carboxylate compounds designed to be decomposed at temperatures between 110 and 170°C . Figure 2.15 shows the appearance change of a Ag carboxylate droplet during heating. Ag carboxylates are expected to be one of the metallic inks or of the sintering aids for other metallic particles. The percentages of Ag in the compounds are in the range of 30–50wt%. Excellent electric resistance (e.g., $10^{-5} \Omega\text{cm}$), lower than that of commercial Ag nanopaste, was achieved at a curing temperature of 160°C .

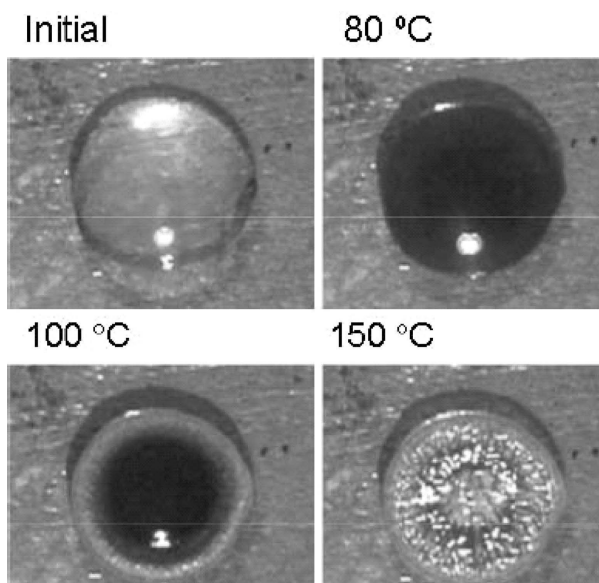


Fig. 2.15. Appearance change of an Ag carboxylate droplet during heating

Room temperature wiring is one of the last goals for printed electronics. room temperature fabrication enables to use the wide variety of functional materials into one circuit board without thermal stress or damage as well as environmental consciousness. Metallic nanoparticles can be sintered to form dense microstructure if both the surface of nanoparticles and the environment are clean without any oxidation or contamination. Ag nanoparticles are, however, usually protected by an organic layer. It is desirable to remove this organic layer by certain chemical processes with or without light heating or other kinds of energy processes, which do not have any serious damage on organic devices and substrates weak against heating.

Recently, the authors developed a new process, by which the paste of Ag nanoparticles protected with them can be successfully sintered at room temperature in air atmosphere. One of the typical organic layer is dodecylamine. In order to remove the dodecylamine layer, it was found that alcohol treatment is quite effective. For instance, Ag nanoparticles ink was printed into lines on a glass substrate and it was dipped into methanol for 10–7,200 s. As a result, sintering was immediately started and resultant Ag wires exhibited excellent low resistivity, $7.3 \times 10^{-5} \Omega\text{cm}$ after 7,200 s dipping. Microstructural observation on this room temperature sintering revealed that, as dipping time gets longer, Ag nanoparticles agglomerate coarsened and connection among particles becomes clearer even in a few

minutes. Thus, a novel room temperature wiring method for Ag nanoparticles has been successfully developed in air atmosphere.

2.7 Nanowires and Nanobelts

2.7.1 Introduction

A nanowire is a wire of diameter of the order of a nanometer (10^{-9} m). Alternatively, nanowires can be defined as structures that have a lateral size constrained to tens of nanometers or less and an unconstrained longitudinal size. At these scales, quantum mechanical effects are important, and hence such wires are also known as “quantum wires.” Many different types of nanowires exist, including metallic (e.g., Ni, Pt, Au) [137], semiconducting (e.g., Si, InP, GaN, ZnO) [138], and insulating (e.g., SiO_2 , TiO_2) [139]. Molecular nanowires are composed of repeating molecular units either organic (e.g., DNA) or inorganic (e.g., $\text{Mo}_6\text{S}_{9-x}\text{I}_x$) [140].

A common technique for creating a nanowire is the vapor–liquid–solid (VLS) synthesis method [141–143]. This technique uses as source material either laser ablated particles or a feed gas. The source is then exposed to a catalyst. For nanowires, the best catalysts are liquid metal (such as gold) nanoclusters, which can either be purchased in colloidal form or by electron-beam deposition and deposited on a substrate or self-assembled from a thin film by dewetting. This process can often produce crystalline nanowires in the case of semiconductor materials. The source enters these nanoclusters and begins to saturate it. Once supersaturation is reached, the source solidifies and grows outward from the nanocluster. The final length of the nanowires can be adjusted by simply turning off the source. Compound nanowires with super-lattices of alternating materials can be created by switching sources while still in the growth phase.

Nanowires (NWs) and nanobelts (NBs) have been demonstrated as building blocks for fabricating nanodevices, such as FET [144], gas sensor [145], diodes [146], LED [147], biosensors [148–150].

2.7.2 Applications of Nanowires

Perhaps the most obvious use for nanowires is in electronics. Some nanowires are very good conductors or semiconductors, and their minis-

cule size means that manufacturers could fit millions more transistors on a single microprocessor. As a result, computer speed would increase dramatically.

Nanowires may play an important role in the field of quantum computers. Doh et al. in the Netherlands created nanowires out of indium arsenide and attached them to aluminum electrodes [151]. At temperatures near absolute zero, aluminum becomes a superconductor, meaning it can conduct electricity without any resistance. The nanowires also became superconductors due to the proximity effect. The researchers could control the superconductivity of the nanowires by running various voltages through the substrate under the wires.

Nanowires may also play an important role in nano-size devices like nanorobots. Doctors could use the nanorobots to treat diseases like cancer. Some nanorobot designs have onboard power systems, which would require structures like nanowires to generate and conduct power.

Using piezoelectric material, nanoscientists could create nanowires that generate electricity from kinetic energy. The piezoelectric effect is a phenomenon certain materials exhibit – when you apply physical force to a piezoelectric material, it emits an electric charge. If you apply an electric charge to this same material, it vibrates. Piezoelectric nanowires might provide power to nano-size systems in the future, though at present there are no practical applications.

There are hundreds of other potential nanowire applications in electronics. Researchers in Japan are working on atomic switches that might some day replace semiconductor switches in electronic devices [152]. Scientists with the National Renewable Energy Laboratory hope that coaxial nanowires will improve the energy efficiency of solar cells [153].

2.7.2.1 Application of Nanowire in Sensor Technology

Pd as the active sensing material has unique property of interaction with hydrogen gas. Partial pressure change of hydrogen gas determines Pd's physical properties (mass, volume, electrical resistance) by forming Pd-H hydride. The difference of electrical resistance by the partial pressure change of hydrogen gas is used as the signal of hydrogen sensor. However, pure palladium has issues in sensor application such as slow response time and high detecting limit [154]. Nano-sized material has large surface-to-volume ratio for hydrogen sensing and advantages for improvement of sensor performance. Palladium nanowire has been the subject of intense interest as sensor materials and structures [155].

Yun et al. [156] demonstrated the fabrication technique involves electrodeposition to directly grow nanowires between patterned thin-film contact electrodes (Fig. 2.16). To demonstrate nanowire sensors, the author

electrochemically grown metal (Pd, Au, Pt), metal oxide (Sb_2O_3), and conducting polymer (polyaniline)-bundled nanowires. Using Pt-bundled nanowires surface modified with glucose oxidase, the author demonstrated glucose detection as a demonstration of a biomolecular sensor.

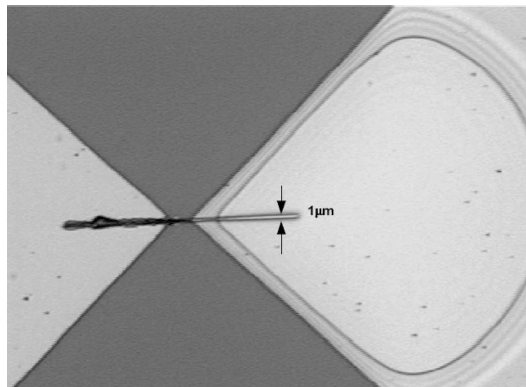


Fig. 2.16. An optical image of electrodeposited Pd wires grown between electrodes for biomedical sensor application [156]

Lee et al. [157] investigated the application of Pd–Ag nanowires as hydrogen sensor. The wire or dendrite-shaped Ag nanowire was grown by electrochemical migration method in a few minutes. The diameter of this nanowire is 50 ~ 200 nm. Pd–Ag nanowire was fabricated using Pd thin film evaporated on the Ag nanowire with 20 – 500 nm thickness. This structure can provide large surface area for sensor. The large surface area gives the reaction sites between Pd–Ag nanowire and hydrogen gas to reduce response time and increase sensitivity. The response time of Pd–Ag nanowire (with 20 nm thickness of the Pd film) is about 5 s at room temperature. The response time and sensitivity are increased according to the thickness of the Pd film on Ag nanowire. Pd–Ag nanowire is saturated and responds easily at lower concentration of hydrogen gas. The Pd film on Ag nanowire did not show the peel-off phenomenon, while pure Pd film is separated from substrate after sensing test. The mechanical stress brings this phenomenon is released by evaporating Pd film on the Ag nanowire mesh.

2.7.2.2 Nanogenerator from ZnO Nanowires

Developing novel technologies for wireless nanodevices and nanosystems is of critical importance for in situ, real-time, and implantable biosensing, remote and wireless sensing, defense technology, and commercial applications. The power sources required by such devices are highly desired to be

lifetime self-charging and in comparable small sizes. Harvesting energy from environment, including solar, thermal, and mechanical energies, provides a perfect solution for these applications. There are huge emergent needs for nanoscale sensing devices for biological sensing and defense applications. Among those possible energy sources, mechanical wave and vibration energies more ubiquitously exist under various circumstances around us [158]. Relying on the piezoelectric effect of a ceramic beam when driven to vibrate by a small mass via gravitation, mechanical energy can be converted into electricity. Many types of MEMS microgenerator have been developed using piezoelectric thin-film cantilevers [159]. However, their relatively large size, bio-incompatible nature, and low sensitivity to small vibrations seriously restrict the application in nanotechnologies and the advantages provided by nano-materials.

Nanowires (NWs) and nanobelts (NBs) of inorganic materials are the forefront in today's nanotechnology research [160]. Among the known one-dimensional nano-materials, zinc oxide (ZnO) has three key advantages [161]. First, it exhibits both semiconducting and piezoelectric properties, providing a unique material for building electro-mechanical coupled sensors and transducers [162, 163]. Second, ZnO is relatively biosafe and biocompatible, and it can be used for biomedical applications with little toxicity. Finally, ZnO exhibits the most diverse and abundant configurations of nanostructures, such as nanowires, nanobelts, nanosprings, nanorings, nanobows, and nanohelices [164]. Recently, Wang et al. at Georgia Tech developed a novel approach of converting mechanical energy into electric power using aligned ZnO nanowires. This discovery sets the foundation for nanoscale power conversion, which will potentially lead to a new adaptable, mobile, and cost-effective energy harvesting technology [165–168].

The piezoelectric nanogenerators are built on vertically aligned ZnO NWs. The operation principle relies on the piezoelectric potential generated on a bent ZnO NW. The rectifying effect of the Schottky junction between the metal electrode and the ZnO crystal can selectively accumulate and release charging, resulting in a continuous mechanical-to-electric energy conversion. The nanogenerator can convert small mechanical vibration energy and hydraulic energy into electricity under various circumstances, such as under ground, in water, or even inside human body. Wang et al. have developed an innovative approach by using ultrasonic waves to drive the motion of the NWs, leading to the production of a continuous current (Fig. 2.17) [169]. The nanogenerator worked continuously for an extended period of time of beyond 1 h. The authors were able to increase the output current to 800 nA and voltage to 10 mV.

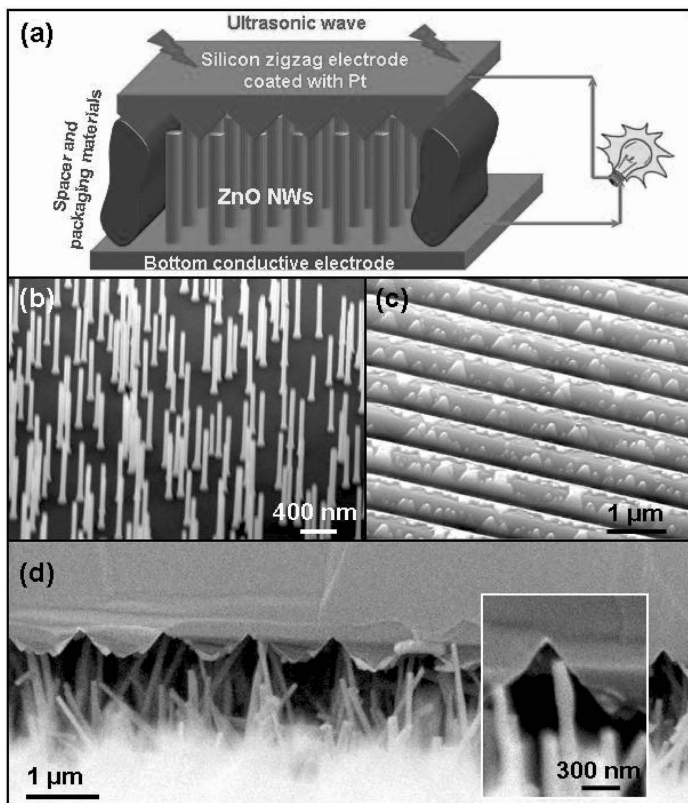


Fig. 2.17. Nanogenerators driven by an ultrasonic wave. (a) Schematic diagram showing the design and structure of the nanogenerator. (b) Low-density aligned ZnO NWs grown on a GaN substrate. (c) Zigzag trenced electrode coated with Pt. (d) Cross-sectional SEM image of the nanogenerator. Inset: A typical NW that is forced by the electrode to bend [169]

The application and the energy conversion efficiency largely depend on the fabrication and packaging techniques. In general, majority of the NWs (ideally 100%) need to be involved in power generation and all the NWs have to be well isolated from the corrosive surroundings but still have free movement. This requires a high dimensional uniformity of the NWs as well as a perfect positioning and alignment of the top electrode on the NW arrays. Upon addressing these crucial challenges, the nanogenerators can potentially become a new self-powered technology for lifetime unattended sensor systems, battery-free electronics, and even in situ, real-time, and implantable biological devices.

References

- [1] H. W. C. Postma, T. Teepen, Z. Yao, M. Grifoni, and C. Dekker, "Carbon Nanotube Single-Electron Transistors at Room Temperature," *Science*, 293, 76–79, 2001.
- [2] J. Xiang, W. Lu, Y. J. Hu, Y. Wu, H. Yan, and C. M. Lieber, "Ge/Si Nanowire Heterostructures as High-Performance Field-Effect Transistors," *Nature*, 441, 489–493, 2006.
- [3] M. C. Petty, M. R. Bryce, and D. Bloor, "An Introduction to Molecular Electronics," Edward Arnold, London, 1995.
- [4] A. Aviram and M. A. Ratner, "Molecular Rectifier," *Chemical Physics Letters*, 29, 277, 1974.
- [5] A. Aviram, "Molecules for Memory, Logic, and Amplification," *Journal of the American Chemical Society*, 110, 5687–5692, 1988.
- [6] J. E. Morris, "Nanopackaging: Nanotechnologies and Electronics Packaging," Springer, Berlin, 2008.
- [7] S. H. Sun, C. B. Murray, D. Weller, L. Folks, and A. Moser, "Monodisperse FePt Nanoparticles and Ferromagnetic FePt Nanocrystal Superlattices," *Science*, 287, 1989–1992, 2000.
- [8] K. W. Park, J. H. Choi, B. K. Kwon, S. A. Lee, Y. E. Sung, H. Y. Ha, S. A. Hong, H. Kim, and A. Wieckowski, "Chemical and Electronic Effects of Ni in Pt/Ni and Pt/Ru/Ni Alloy Nanoparticles in Methanol Electrooxidation," *Journal of Physical Chemistry B*, 106, 1869–1877, 2002.
- [9] M. P. Mallin and C. J. Murphy, "Solution-Phase Synthesis of Sub-10 nm Au-Ag Alloy Nanoparticles," *Nano Letters*, 2, 1235–1237, 2002.
- [10] A. Henglein and M. Giersig, "Radiolytic Formation of Colloidal Tin and Tin-Gold Particles in Aqueous-Solution," *Journal of Physical Chemistry*, 98, 6931–6935, 1994.
- [11] P. Lu, J. Dong, and N. Toshima, "Surface-Enhanced Raman Scattering of a Cu/Pd Alloy Colloid Protected by Poly(N-vinyl-2-pyrrolidone)," *Langmuir*, 15, 7980–7992, 1999.
- [12] S. Link, C. Burda, Z. L. Wang, and M. A. El-Sayed, "Electron Dynamics in Gold and Gold-Silver Alloy Nanoparticles: The Influence of a Nonequilibrium Electron Distribution and the Size Dependence of the Electron-Phonon Relaxation," *Journal of Chemical Physics*, 111, 1255–1264, 1999.
- [13] Y. B. Zhao, Z. J. Zhang, and H. X. Dang, "Synthesis of In-Sn Alloy Nanoparticles by a Solution Dispersion Method," *Journal of Materials Chemistry*, 14, 299–302, 2004..
- [14] Y. H. Chen and C. S. Yeh, "A New Approach for the Formation of Alloy Nanoparticles: Laser Synthesis of Gold-Silver Alloy from

- Gold-Silver Colloidal Mixtures,” *Chem. Commun.*, 4, 371–372, 2001.
- [15] J. Zhang, J. Worley, S. Denomme, C. Kingston, Z. J. Jakubek, Y. Deslandes, M. Post, B. Simard, N. Braidy, and G. A. Botton, “Synthesis of Metal Alloy Nanoparticles in Solution by Laser Irradiation of a Metal Powder Suspension,” *Journal of Physical Chemistry B*, 107, 6920–6923, 2003.
- [16] M. Mandal, N. R. Jana, S. Kundu, S. K. Ghosh, M. Panigrahi, and T. Pal, “Synthesis of Au-core-Ag-shell Type Bimetallic Nanoparticles for Single Molecule Detection in Solution by SERS Method,” *Journal of Nanoparticle Research*, 6, 53–61, 2004.
- [17] G. Southam and T. J. Beveridge, “The Occurrence of Sulfur and Phosphorus within Bacterially Derived Crystalline and Pseudocrystalline Octahedral Gold Formed in vitro,” *Geochimica Et Cosmochimica Acta*, 60, 4369–4376, 1996.
- [18] D. Fortin and T. J. Beveridge, From Biology to Biotechnology and Medical Applications, in *Biomineralization*, E. Baeuerien, Ed., Wiley-VCH, Weinheim, pp. 7, 2000.
- [19] T. Klaus, R. Joerger, E. Olsson, and C. G. Granqvist, “Silver-Based Crystalline Nanoparticles, Microbially Fabricated,” *Proceedings of the National Academy of Sciences of the United States of America*, vol. 96, pp. 13611–13614, 1999.
- [20] T. Klaus-Joerger, R. Joerger, E. Olsson, and C. G. Granqvist, “Bacteria as Workers in the Living Factory: Metal-Accumulating Bacteria and their Potential for Materials Science,” *Trends in Biotechnology*, 19, 15–20, 2001.
- [21] R. Joerger, T. Klaus, and C. G. Granqvist, “Biologically Produced Silver-Carbon Composite Materials for Optically Functional Thin-Film Coatings,” *Advanced Materials*, 12, 407–409, 2000.
- [22] B. Nair and T. Pradeep, “Coalescence of Nanoclusters and Formation of Submicron Crystallites Assisted by Lactobacillus Strains,” *Crystal Growth & Design*, 2, 293–298, 2002.
- [23] J. L. Gardea-Torresdey, J. G. Parsons, E. Gomez, J. Peralta-Videa, H. E. Troiani, P. Santiago, and M. J. Yacaman, “Formation and Growth of Au Nanoparticles Inside Live Alfalfa Plants,” *Nano Letters*, 2, 397–401, 2002.
- [24] J. L. Gardea-Torresdey, E. Gomez, J. R. Peralta-Videa, J. G. Parsons, H. Troiani, and M. Jose-Yacaman, “Alfalfa Sprouts: A Natural Source for the Synthesis of Silver Nanoparticles,” *Langmuir*, 19, 1357–1361, 2003.
- [25] M. Ohring, “Materials Science of Thin Films: Deposition & Structure,” 2nd Ed., Academic Press, pp. 395–397, 2002.

- [26] J. E. Morris, "Single-Electron Transistors," in *The Electrical Engineering Handbook Third edition: Electronics, Power Electronics, Optoelectronics, Microwaves, Electromagnetics, and Radar*, Richard C. Dorf, Ed., CRC/Taylor & Francis, Boca Raton, FL, pp. 3.53–3.64, 2006.
- [27] J. Xu and C. P. Wong, "High-K Nanocomposites with Core-Shell Structured Nanoparticles for Decoupling Applications," *Proceedings of the 55th IEEE Electronic Component & Technology Conference*, pp. 1234–1240, 2005.
- [28] F. Wu and J. E. Morris, "Characterizations of $(\text{SiO}_x\text{Cr}_{1-x})\text{N}_{1-y}$ Thin Film Resistors for Integrated Passive Applications," *53rd Electronic Components & Technology Conference*, pp. 161–166, 2003.
- [29] J. E. Morris, "Recent Developments in Discontinuous Metal Thin Film Devices," *Vacuum*, 50, 107–113, 1998.
- [30] J. E. Morris, F. Wu, C. Radehaus, M. Hietschold, A. Henning, K. Hofmann, and A. Kiesow, "Single Electron Transistors: Modeling and Fabrication," *Proceedings of the 7th International Conference Solid State & Integrated Circuit Technology (ICSICT)*, Beijing, pp. 634–639, 2004.
- [31] H. Jiang, K. Moon, H. Dong, and F. Hua, "Thermal Properties of Oxide Free Nano Non Noble Metal for Low Temperature Interconnect Technology," *Proceedings of the 56th IEEE Electronic Component & Technology Conference*, San Diego, CA, pp. 1969–1973, 2006.
- [32] R. A. Flinn and P. K. Trojan, "Engineering Materials & their Applications," 2nd Ed., Houghton-Mifflin, Boston, MA, pp. 75–77, 1981.
- [33] T. Yamaguchi, M. Sakai, and N. Saito, "Optical-Properties of Well-Defined Granular Metal Systems," *Physical Review B*, 32, 2126–2131, 1985.
- [34] R. Das, M. Poliks, J. Lauffer, and V. Markovich, "High Capacitance, Large Area, Thin Film, Nanocomposite Based Embedded Capacitors," *Proceedings of the 56th IEEE Electronic Component & Technology Conference*, San Diego, CA, pp. 1510–1515, 2006.
- [35] J. Xu and C. P. Wong, "Effects of the Low Loss Polymers on the Dielectric Behavior of Novel Aluminum-Filled High-k Nanocomposites," *Proceedings of the 54th IEEE Electronic Component & Technology Conference*, Las Vegas, pp. 496–506, 2004.
- [36] J. Lu, K. Moon, and C. P. Wong, "Development of Novel Silver Nanoparticles/Polymer Composites as High K Polymer Matrix by In-Situ Photochemical Method," *Proceedings of the 56th IEEE*

- Electronic Component & Technology Conference*, San Diego, CA, pp. 1841–1846, 2006.
- [37] L. Ekstrand, H. Kristiansen, and J. Liu, “Characterization of Thermally Conductive Epoxy Nano Composites,” *Proceedings of the 28th International Spring Seminar on Electronics Technology (ISSE'05)*, Vienna, 2005.
- [38] L. Fan, B. Su, J. Qu, and C. P. Wong, “Electrical and Thermal Conductivities of Polymer Composites Containing Nano-Sized Particles,” *Proceedings of the 54th IEEE Electronic Component & Technology Conference*, Las Vegas, NV, pp. 148–154, 2004.
- [39] H. Jiang, K. Moon, L. Zhu, J. Lu, and C. P. Wong, “The Role of Self-Assembled Monolayer (SAM) on Ag Nanoparticles for Conductive Nanocomposite,” *Proceedings of the 10th IEEE/CPMT International Symposium on Advanced Packaging Materials*, Irvine, CA, pp. 266–271, 2005.
- [40] R. Das, J. Lauffer, and F. Egitto, “Electrical Conductivity and Reliability of Nano- and Micro-Filled Conducting Adhesives for Z-axis Interconnections,” *Proceedings of the 56th IEEE Electronic Component & Technology Conference*, San Diego, CA, pp. 112–118, 2006.
- [41] K. Moon, S. Pothukuchi, Y. Li, and C. P. Wong, “Nano Metal Particles for Low Temperature Interconnect Technology,” *Proceedings of the 54th IEEE Electronic Component & Technology Conference*, Las Vegas, NV, pp. 1983–1988, 2004.
- [42] P. Lall, S. Islam, J. Suhling, and G. Tian, “Nano-Underfills for High-Reliability Applications in Extreme Environments,” *Proceedings of the 55th IEEE Electronic Component & Technology Conference*, Orlando, FL, pp. 212–222, 2005.
- [43] Y. Li, K. S. Moon, and C. P. Wong, “Adherence of Self-Assembled Monolayers on Gold and Their Effects for High-Performance Anisotropic Conductive Adhesives,” *Journal of Electronic Materials*, 34, 266–271, 2005.
- [44] S. Joo and D. F. Baldwin, “Demonstration for Rapid Prototyping of Micro-Systems Packaging by Data-Driven Chip-First Processing Using Nano-Particles Metal Colloids,” *Proceedings of the 55th IEEE Electronic Component & Technology Conference*, Orlando, FL, PP. 1859–1863, 2005.
- [45] A. Moscicki, J. Felba, T. Sobierajski, J. Kudzia, A. Arp, and W. Meyer, “Electrically Conductive Formulations Filled Nano Size Silver Filler for Ink-Jet Technology,” *Proceedings of the 5th International Conference on Polymers and Adhesives in Microelectronics and Photonics*, Wroclaw, Poland, pp. 40–44, 2005.

- [46] J. Kolbe, A. Arp, F. Calderone, E. M. Meyer, W. Meyer, H. Schaefer, and M. Stuve, "Inkjettable Conductive Adhesive for Use in Microelectronics and Microsystems Technology," *Proceedings of the 5th International Conference on Polymers and Adhesives in Microelectronics and Photonics*, Wroclaw, Poland, pp. 160–163, 2005.
- [47] J. G. Bai, K. D. Creehan, and H. A. Kuhn, "Inkjet Printable Nanosilver Suspensions for Enhanced Sintering Quality in Rapid Manufacturing," *Nanotechnology*, 18, 1–5, 2007.
- [48] W. Peng, V. Hurskainen, K. Hashizume, S. Dunford, S. Quander, and R. Vatanparast, "Flexible Circuit Creation with Nano Metal Particles," *Proceedings of the 55th IEEE Electronic Component & Technology Conference*, Orlando, FL, pp. 77–82, 2005.
- [49] J. G. Bai, Z. Z. Zhang, J. N. Calata, and G. Q. Lu, "Low-Temperature Sintered Nanoscale Silver as a Novel Semiconductor Device-Metallized Substrate Interconnect Material," *IEEE Transactions on Components and Packaging Technologies*, 29, 589–593, 2006.
- [50] D. Wakuda, M. Hatamura, and K. Suganuma, "Novel Room Temperature Wiring Process of Ag Nanoparticle Paste," *Proceedings of the 6th International Conference on Polymers and Adhesives in Microelectronics and Photonics*, Tokyo, pp. 110–113, 2007.
- [51] A. Moscicki, J. Felba, P. Gwiazdzinski, and M. Puchalski, "Conductivity Improvement of Microstructures Made by Nano-Size-Silver Filled Formulations," *Proceedings of the 6th International Conference on Polymers and Adhesives in Microelectronics and Photonics*, Tokyo, pp. 305–310, 2007.
- [52] J. G. Bai, Z. Z. Zhang, J. N. Calata, and G. Q. Lu, "Characterization of Low-Temperature Sintered Nanoscale Silver Paste for Attaching Semiconductor Devices," *Proceedings of the 7th IEEE CPMT Conference on High Density Microsystem Design and Packaging and Component Failure Analysis (HDP'05)*, Shanghai, pp. 272–276, 2005.
- [53] Y. Sun, Z. Zhang, and C. P. Wong, "Photo-Definable Nanocomposite for Wafer Level Packaging," *Proceedings of the 55th IEEE Electronic Component & Technology Conference*, Orlando, FL, pp. 179–184, 2005.
- [54] Y. Sun and C. P. Wong, "Study and Characterization on the Nanocomposite Underfill for Flip Chip Applications," *Proceedings of the 54th IEEE Electronic Component & Technology Conference*, Las Vegas, NV, pp. 477–483, 2004.
- [55] Y. Sun, Z. Zhang, and C. P. Wong, "Fundamental Research on Surface Modification of Nano-Size Silica for Underfill Applica-

- tions,” *Proceedings of the 54th IEEE Electronic Component & Technology Conference*, Las Vegas, NV, pp. 754–760, 2004.
- [56] M. Roy, J. K. Nelson, R. K. MacCrone, L. S. Schadler, C. W. Reed, R. Keefe, and W. Zenger, “Polymer Nanocomposite Dielectrics – The Role of the Interface,” *IEEE Transactions on Dielectrics and Electrical Insulation*, 2, 629–643, 2005.
- [57] W. Guan, S. C. Verma, Y. Gao, C. Andersson, Q. Zhai, and J. Liu, “Characterization of Nanoparticles of Lead Free Solder Alloys,” *Proceedings of the 1st IEEE Electronics Systemintegration Technology Conference*, Dresden, Germany, 2006.
- [58] K. M. Kumar, V. Kripesh, and A. A. O. Tay, “Sn-Ag-Cu Lead-free Composite Solders for Ultra-Fine-Pitch Wafer-Level Packaging,” *Proceedings of the 56th IEEE Electronic Component & Technology Conference*, San Diego, CA, pp. 237–243, 2006.
- [59] M. Amagai, “A Study of Nano Particles in SnAg-Based Lead Free Solders for Intermetallic Compounds and Drop Test Performance,” *Proceedings of the 56th IEEE Electronic Component & Technology Conference*, San Diego CA, pp. 1170–1190, 2006.
- [60] V. Kripesh, K. Mohankumar, and A. Tay, “Properties of Solders Reinforced with Nanotubes and Nanoparticles,” *Proceedings of the 56th IEEE Electronic Component & Technology Conference*, San Diego, CA, 2006.
- [61] K. M. Klein, J. Zheng, A. Gewirtz, D. S. Sarma, S. Rajalakshmi, and S. K. Sitaraman, “Array of Nano-Cantilevers as a Bio-Assay for Cancer Diagnosis,” *Proceedings of the 55th IEEE Electronic Component & Technology Conference*, Orlando, FL, pp. 583–587, 2005.
- [62] H. Jiang, K. S. Moon, F. Hua, and C. P. Wong, “Synthesis and Thermal and Wetting Properties of Tin/Silver Alloy Nanoparticles for Low Melting Point Lead-free Solders,” *Chemistry of Materials*, 19, 4482–4485, 2007.
- [63] R. Garrigos, P. Cheyssac, and R. Kofman, “Melting for Lead Particles of Very Small Sizes – Influence of Surface Phenomena,” *Zeitschrift Fur Physik D-Atoms Molecules and Clusters*, 12, 497–500, 1989.
- [64] W. Y. Hu, S. G. Xiao, J. Y. Yang, and Z. Zhang, “Melting Evolution and Diffusion Behavior of Vanadium Nanoparticles,” *European Physical Journal B*, 45, 547–554, 2005.
- [65] W. Guan, S. C. Verma, Y. Gao, C. Andersson, Q. Zhai, and J. Liu, “Characterization of Nanoparticles of Lead Free Solder Alloys,” *Electronics Systemintegration Technology Conference*, vol. 1, pp. 7–12, 2006.

- [66] Z. W. Li, X. J. Tao, Y. M. Cheng, Z. S. Wu, Z. J. Zhang, and H. X. Dang, "A Facile Way for Preparing Tin Nanoparticles from Bulk Tin via Ultrasound Dispersion," *Ultrasonics Sonochemistry*, 14, 89–92, 2007.
- [67] Y. B. Zhao, Z. J. Zhang, and H. X. Dang, "A Simple Way to Prepare Bismuth Nanoparticles," *Materials Letters*, 58, 790–793, 2004.
- [68] H. J. Chen, Z. W. Li, Z. S. Wu, and Z. J. Zhang, "A Novel Route to Prepare and Characterize Sn-Bi Nanoparticles," *Journal of Alloys and Compounds*, 394, 282–285, 2005.
- [69] K. Mohankumar and A. A. O. Tay, "Nanoparticle Reinforced Solders for Fine Pitch Applications," *Proceedings of Electronics Packaging Technology Conference*, pp. 455–461, 2006.
- [70] K. M. Kumar, "Sn-Ag-Cu Lead-free Composite Solders for Ultra-Fine-Pitch Wafer-Level Packaging," *Proceedings of the 56th IEEE Electronic Component & Technology Conference*, San Diego, CA, pp. 237–243, 2006.
- [71] F. Qi, L. Sun, Z. Hou, J. Wang, and C. Qin, *International Conference on Electronic Packaging Technology & High Density Packaging*, pp. 1–3, 2008.
- [72] M. Amagai, "A Study of Nanoparticles in Sn-Ag Based Lead Free Solders," *Microelectronics Reliability*, 48, 1–16, 2008.
- [73] G. E. Moore, "Progress in Digital Integrated Electronics," *International Electron Devices Meetings*, Washington D. C., pp. 11–13, 1975.
- [74] F. Kreupl, A. P. Graham, G. S. Duesberg, W. Steinhogel, M. Liebau, E. Unger, and W. Honlein, "Carbon Nanotubes in Interconnect Applications," *Microelectronic Engineering*, 64, 399–408, 2002.
- [75] A. P. Graham, G. S. Duesberg, W. Hoenlein, F. Kreupl, M. Liebau, R. Martin, B. Rajasekharan, W. Pamler, R. Seidel, W. Steinhogel, and E. Unger, "How Do Carbon Nanotubes Fit into the Semiconductor Roadmap?," *Applied Physics A-Materials Science & Processing*, 80, 1141–1151, 2005.
- [76] S. Frank, P. Poncharal, Z. L. Wang, and W. A. de Heer, "Carbon Nanotube Quantum Resistors," *Science*, 280, 1744–1746, 1998.
- [77] T. M. Wu and E. C. Chen, "Crystallization Behavior of Poly(epsilon-caprolactone)/Multiwalled Carbon Nanotube Composites," *Journal of Polymer Science Part B-Polymer Physics*, 44, 598–606, 2006.
- [78] S. Mizuno, A. Verma, H. Tran, P. Lee, and B. Nguyen, "Dielectric Constant and Stability of Fluorine Doped PECVD Silicon Oxide Thin Films," *Thin Solid Films*, 283, 30–36, 1996.

- [79] B. Q. Wei, R. Vajtai, and P. M. Ajayan, "Reliability and Current Carrying Capacity of Carbon Nanotubes," *Applied Physics Letters*, 79, 1172–1174, 2001.
- [80] A. P. Graham, G. S. Duesberg, R. V. Seidel, M. Liebau, E. Unger, W. Pamler, F. Kreupl, and W. Hoenlein, "Carbon Nanotubes for Microelectronics?," *Small*, 1, 382–390, 2005.
- [81] M. Nihei, A. Kawabata, D. Kondo, M. Horibe, S. Sato, and Y. Awano, "Electrical Properties of Carbon Nanotube Bundles for Future via Interconnects," *Japanese Journal of Applied Physics Part 1-Regular Papers Short Notes & Review Papers*, 44, 1626–1628, 2005.
- [82] W. Hoenlein, F. Kreupl, G. S. Duesberg, A. P. Graham, M. Liebau, R. Seidel, and E. Unger, "Carbon Nanotubes for Microelectronics: Status and Future Prospects," *Materials Science & Engineering C-Biomimetic and Supramolecular Systems*, 23, 663–669, 2003.
- [83] Y. Awano, "Carbon Nanotube Technologies for LSI via Interconnects," *IEICE Trans. Electron.*, E89C, 1499–1503, 2006.
- [84] L. B. Zhu, Y. Y. Sun, D. W. Hess, and C. P. Wong, "Well-aligned Open-ended Carbon Nanotube Architectures: An Approach for Device Assembly," *Nano Letters*, 6, 243–247, 2006.
- [85] A. Naeemi, G. Huang, and J. Meindl, "Performance Modeling for Carbon Nanotube Interconnects in On-chip Power Distribution," *Proceedings of the 57th IEEE Electronic Component & Technology Conference*, Reno, NV, pp. 420–428, 2007.
- [86] Y. Chai, J. Gong, K. Zhang, P. C. H. Chan, and M. M. F. Yuen, "Low Temperature Transfer of Aligned Carbon Nanotube Films Using Liftoff Technique," *Proceedings of the 57th IEEE Electronic Component & Technology Conference*, Reno, NV, pp. 429–434, 2007.
- [87] C.-J. Wu, C.-Y. Chou, C.-N. Han, and K.-N. Chiang, "Simulation and Validation of CNT Mechanical Properties – The Future Interconnection Method," *Proceedings of the 57th IEEE Electronic Component & Technology Conference*, Reno, NV, pp. 447–452, 2007.
- [88] A. Ruiz, E. Vega, R. Katiyar, and R. Valentin, "Novel Enabling Wire Bonding Technology," *Proceedings of the 57th IEEE Electronic Component & Technology Conference*, Reno, NV, pp. 458–462, 2007.
- [89] G. A. Riley, "Nanobump Flip Chips," *Advanced Packaging*, 18–20, April, 2007.
- [90] R. T. Pike, R. Dellmo, J. Wade, S. Newland, G. Hyland, and C. M. Newton, "Metallic Fullerene and MWCNT Composite Solutions

- for Microelectronics Subsystem Electrical Interconnection Enhancement,” *Proceedings of the 54th IEEE Electronic Component & Technology Conference*, Las Vegas, NV, pp. 461–465, 2004.
- [91] J. Ding, S. Rea, D. Linton, E. Orr, and J. MacConnell, “Mixture Properties of Carbon Fibre Composite Materials for Electronics Shielding in Systems Packaging,” *Proceedings of the 1st IEEE Electronics Systemintegration Technology Conference*, Dresden, Germany, pp. 19–25, 2006.
- [92] J.-C. Chiu, C.-M. Chang, W.-H. Cheng, and W.-S. Jou, “High-Performance Electromagnetic Susceptibility for a 2.5Gb/s Plastic Transceiver Module Using Mutli-Wall Carbon Nanotubes,” *Proceedings of the 56th IEEE Electronic Component & Technology Conference*, San Diego, CA, pp. 183–186, 2006.
- [93] S. Berber, Y. K. Kwon, and D. Tomanek, “Unusually High Thermal Conductivity of Carbon Nanotubes,” *Physical Review Letters*, 84, 4613–4616, 2000.
- [94] E. Pop, D. Mann, Q. Wang, K. Goodson, and H. J. Dai, “Thermal Conductance of an Individual Single-wall Carbon Nanotube above Room Temperature,” *Nano Letters*, 6, 96–100, 2006.
- [95] P. Kim, L. Shi, A. Majumdar, and P. L. McEuen, “Thermal Transport Measurements of Individual Multiwalled Nanotubes,” *Physical Review Letters*, 87, 215502-1–215502-4, 2001.
- [96] J. Hone, M. C. Llaguno, N. M. Nemes, A. T. Johnson, J. E. Fischer, D. A. Walters, M. J. Casavant, J. Schmidt, and R. E. Smalley, “Electrical and Thermal Transport Properties of Magnetically Aligned Single Wall Carbon Nanotube Films,” *Applied Physics Letters*, 77, 666–668, 2000.
- [97] W. Yi, L. Lu, D. L. Zhang, Z. W. Pan, and S. S. Xie, “Linear Specific Heat of Carbon Nanotubes,” *Physical Review B*, 59, R9015–R9018, 1999.
- [98] D. J. Yang, Q. Zhang, G. Chen, S. F. Yoon, J. Ahn, S. G. Wang, Q. Zhou, Q. Wang, and J. Q. Li, “Thermal Conductivity of Multiwalled Carbon Nanotubes,” *Physical Review B*, 66, 165440.1–165440.6, 2002.
- [99] J. Xu and T. S. Fisher, “Enhancement of Thermal Interface Materials with Carbon Nanotube Arrays,” *International Journal of Heat and Mass Transfer*, vol49, 1658–1666, 2006.
- [100] Y. Xu, Y. Zhang, E. Suhir, and X. W. Wang, “Thermal Properties of Carbon Nanotube Array Used for Integrated Circuit Cooling,” *Journal of Applied Physics*, 100, 074302, 2006.
- [101] K. Zhang, Y. Chai, M. M. F. Yuen, D. G. W. Xiao, and P. C. H. Chan, “Carbon Nanotube Thermal Interface Material for High-

- Brightness Light-Emitting-Diode Cooling,” *Nanotechnology*, 19, 215706, 2008.
- [102] R. Prasher, “Thermal Interface Materials: Historical Perspective, Status, and Future Directions,” *Proceedings of the IEEE*, vol. 94, pp. 1571–1586, 2006.
 - [103] J. Xu and T. S. Fisher, “Enhanced Thermal Contact Conductance Using Carbon Nanotube Array Interfaces,” *IEEE Transactions on Components and Packaging Technologies*, 29, 261–267, 2006.
 - [104] T.-M. Lee, K.-C. Chiou, F.-P. Tseng, and C.-C. Huang, “High Thermal Efficiency Carbon Nanotube-Resin Matrix for Thermal Interface Materials,” *Proceedings of the 55th IEEE Electronic Component & Technology Conference*, Orlando, FL, pp. 55–59, 2005.
 - [105] J. Liu, M. O. Olorunyomi, X. Lu, W. X. Wang, T. Aronsson, and D. Shangguan, “New Nano-Thermal Interface Material for Heat Removal in Electronics Packaging,” *Proceedings of the 1st IEEE Electronics Systemintegration Technology Conference*, Dresden, Germany, pp. 1–6, 2006.
 - [106] Z. Mo, R. Morjan, J. Anderson, E. E. B. Campbell, and J. Liu, “Integrated Nanotube Microcooler for Microelectronics Applications,” *Proceedings of the 55th IEEE Electronic Component & Technology Conference*, Orlando, FL, pp. 51–54, 2005.
 - [107] L. Ekstrand, Z. Mo, Y. Zhang, and J. Liu, “Modelling of Carbon Nanotubes as Heat Sink Fins in Microchannels for Microelectronics Cooling,” *Proceedings of the 5th International Conference on Polymers and Adhesives in Microelectronics and Photonics*, Wroclaw, Poland, pp. 185–187, 2005.
 - [108] W. Lin, Y. G. Xiu, H. J. Jiang, R. W. Zhang, O. Hildreth, K. S. Moon, and C. P. Wong, “Self-Assembled Monolayer-Assisted Chemical Transfer of In Situ Functionalized Carbon Nanotubes,” *Journal of the American Chemical Society*, 130, 9636–9637, 2008.
 - [109] B. J. Ash, R. W. Siegel, and L. S. Schadler, “Glass-Transition Temperature Behavior of Alumina/PMMA Nanocomposites,” *Journal of Polymer Science Part B-Polymer Physics*, 42, 4371–4383, 2004.
 - [110] W. Peukert, H. C. Schwarzer, M. Gotzinger, L. Gunther, and F. Stenger, “Control of Particle Interfaces – the Critical Issue in Nanoparticle Technology,” *Advanced Powder Technology*, 14, 411–426, 2003.
 - [111] M. F. Fr  chette, M. Trudeau, H. D. Alamdari, and S. Boily, “Introductory Remarks on Nano Dielectrics,” *IEEE Conference on Electrical Insulation and Dielectric Phenomena*, pp. 92–99, 2001.

- [112] B. J. Ash, D. F. Rogers, C. J. Wiegand, L. S. Schadler, R. W. Siegel, B. C. Benicewicz, and T. Apple, "Mechanical Properties of Al₂O₃/Polymethylmethacrylate Nanocomposites," *Polym. Compos.*, 23, 1014–1025, 2002.
- [113] T. Tanaka, G. C. Montanari, and R. Mulhaupt, "Polymer Nanocomposites as Dielectrics and Electrical Insulation-Perspectives for Processing Technologies, Material Characterization and Future Applications," *IEEE Transactions on Dielectrics and Electrical Insulation*, 11, 763–784, 2004.
- [114] T. J. Lewis, "Nanometric Dielectrics," *IEEE Transactions on Dielectrics and Electrical Insulation*, 1, 812–825, 1994.
- [115] M. S. Khalil, P. O. Henk, and M. Henriksen, "The Influence of Titanium Dioxide Additive on the Short-Term DC Breakdown Strength of Polyethylene," *IEEE Intern. Sympos. Electr. Insul., Montreal, Canada*, pp. 268–271, 1990.
- [116] J. K. Nelson and J. C. Fothergill, "Internal Charge Behaviour of Nanocomposites," *Nanotechnology*, 15, 586–595, 2004.
- [117] J. K. Nelson, J. C. Fothergill, and M. Fu, "Dielectric Properties of Epoxy Nanocomposites Containing TiO₂, Al₂O₃ and ZnO Fillers," *IEEE Conference on Electrical Insulation and Dielectric Phenomena*, pp. 406–409, 2004.
- [118] D. L. Ma, R. W. Siegel, J. I. Hong, L. S. Schadler, E. Martensson, and C. Onneby, "Influence of Nanoparticle Surfaces on the Electrical Breakdown Strength of Nanoparticle-Filled Low-Density Polyethylene," *Journal of Materials Research*, 19, 857–863, 2004.
- [119] T. Ramanathan, H. Liu, and L. C. Brinson, "Functionalized SWNT/Polymer Nanocomposites for Dramatic Property Improvement," *Journal of Polymer Science Part B-Polymer Physics*, 43, 2269–2279, 2005.
- [120] J. K. Kim, C. G. Hu, R. S. C. Woo, and M. L. Sham, "Moisture Barrier Characteristics of Organoclay-Epoxy Nanocomposites," *Composites Science and Technology*, 65, 805–813, 2005.
- [121] J. W. Gilman, T. Kashiwagi, and J. D. Lichtenhan, "Nanocomposites: A Revolutionary New Flame Retardant Approach," *Sampe Journal*, 33, 40–46, 1997.
- [122] H. Sharma and Z. Xiao, "Fabrication of Carbon Nanotube Field-Effect Transistors with Metal and Semiconductor Electrodes," in *Nanotubes and Related Nanostructures*, Y. K. Yap, Ed. (*Materials Research Society Symposium Proceedings*), vol. 1057E, 2008.
- [123] N. Srivastava, R. V. Joshi, and K. Banerjee, "Carbon Nanotube Interconnects: Implications for Performance, Power Dissipation and Thermal Management," *IEEE International Electron Devices Meeting*, pp. 249–252, 2005.

- [124] A. Kawabata, S. Sato, T. Nozue, T. Hyakushima, M. Norimatsu, M. Mishima, T. Murakami, D. Kondo, K. Asano, M. Ohfuti, H. Kawarada, T. Sakai, M. Nihei, and Y. Awano, "Robustness of CNT Via Interconnect Fabricated by Low Temperature Process over a High-Density Current," *International Interconnect Technology Conference*, pp. 237–239, 2008.
- [125] I. Soga, D. Kondo, Y. Yamaguchi, T. Iwai, M. Mizukoshi, Y. Awano, K. Yube, and T. Fujii, "Carbon Nanotube Bumps for LSI Interconnect," *Proceedings of Electronic Components and Technology Conference*, pp. 1390–1394, 2008.
- [126] T. Iwai, "Carbon Nanotube Bumps for Thermal and Electrical Conduction in Transistor," *Fujitsu Scientific and Technical Journal*, 43, 508–515, 2007.
- [127] G. Mehrotra, G. Jha, J. D. Goud, P. M. Raj, M. Venkatesan, M. Iyer, D. Hess, and R. Tummala, "Low-Temperature, Fine-Pitch Interconnections Using Self-Patternable Metallic Nanoparticles as the Bonding Layer," *Proceedings of Electronic Components and Technology Conference*, pp. 1410–1416, 2008.
- [128] D. Huang, F. Liao, S. Moles, D. Redinger, and V. Subramanian, "Plastic-Compatible Low Resistance Printable Gold Nanoparticle Conductors for Flexible Electronics," *Journal of the Electrochemical Society*, 150, G412–G417, 2003.
- [129] A. Kamysny, M. Ben-Moshe, S. Aviezer, and S. Magdassi, "Ink-Jet Printing of Metallic Nanoparticles and Microemulsions," *Macromolecular Rapid Communications*, 26, 281–288, 2005.
- [130] A. L. Dearden, P. J. Smith, D. Y. Shin, N. Reis, B. Derby, and P. O'Brien, "A Low Curing Temperature Silver Ink for Use in Ink-Jet Printing and Subsequent Production of Conductive Tracks," *Macromolecular Rapid Communications*, 26, 315–318, 2005.
- [131] Y. H. Byun, E. C. Hwang, S. Y. Lee, Y. Y. Lyu, J. H. Yim, J. Y. Kim, S. Chang, L. S. Pu, and J. M. Kim, "Highly Efficient Silver Patterning without Photo-Resist Using Simple Silver Precursors," *Materials Science and Engineering B-Solid State Materials for Advanced Technology*, 117, 11–16, 2005.
- [132] G. G. Rozenberg, E. Bresler, S. P. Speakman, C. Jeynes, and J. H. G. Steinke, "Patterned Low Temperature Copper-Rich Deposits Using Inkjet Printing," *Applied Physics Letters*, 81, 5249–5251, 2002.
- [133] S. B. Fuller, E. J. Wilhelm, and J. M. Jacobson, "Ink-Jet Printed Nanoparticle Microelectromechanical Systems," *Journal of Microelectromechanical Systems*, 11, 54–60, 2002.
- [134] J. W. Chung, S. W. Ko, N. R. Bieri, C. P. Grigoropoulos, and D. Poulikakos, "Conductor Microstructures by Laser Curing of

- Printed Gold Nanoparticle Ink,” *Applied Physics Letters*, 84, 801–803, 2004.
- [135] D. Kim and J. Moon, “Highly Conductive Ink Jet Printed Films of Nanosilver Particles for Printable Electronics,” *Electrochemical and Solid State Letters*, 8, J30–J33, 2005.
- [136] K. Suganuma, D. Wakuda, M. Hatamura, and K.-S. Kim, “Ink-jet Printing of Nano Materials and Processes for Electronics Applications,” *Proceedings of the IEEE CPMT Conference on High Density Microsystem Design and Packaging and Component Failure Analysis*, 2007.
- [137] D. J. Pena, B. Razavi, P. A. Smith, J. K. Mbindyo, M. J. Natan, T. S. Mayer, T. E. Mallouk, and C. D. Keating, “Electrochemical Synthesis of Multi-Material Nanowires as Building Blocks For Functional Nanostructures,” *MRS Symposium D*, 2000.
- [138] X. F. Duan and C. M. Lieber, “General Synthesis of Compound Semiconductor Nanowires,” *Advanced Materials*, 12, 298–302, 2000.
- [139] B. Xiang, Y. Zhang, Z. Wang, X. H. Luo, Y. W. Zhu, H. Z. Zhang, and D. P. Yu, “Field-Emission Properties of TiO₂ Nanowire Arrays,” *Journal of Physics D-Applied Physics*, 38, 1152–1155, 2005.
- [140] M. I. Ploscaru, S. J. Kokalj, M. Uplaznik, D. Vengust, D. Turk, A. Mrzel, and D. Mihailovic, “Mo₆S_{9-x}I_x Nanowire Recognitive Molecular-scale Connectivity,” *Nano Letters*, 7, 1445–1448, 2007.
- [141] K. K. Lew, L. Pan, E. C. Dickey, and J. M. Redwing, “Vapor-Liquid-Solid Growth of Silicon-Germanium Nanowires,” *Advanced Materials*, 15, 2073–2076, 2003.
- [142] P. Nguyen, S. Vaddiraju, and M. Meyyappan, “Indium and Tin Oxide Nanowires by Vapor-Liquid-Solid Growth Technique,” *Journal of Electronic Materials*, 35, 200–206, 2006.
- [143] S. Bhunia, T. Kawamura, S. Fujikawa, H. Nakashima, K. Furu-kawa, K. Torimitsu, and Y. Watanabe, “Vapor-Liquid-Solid Growth of Vertically Aligned InP Nanowires by Metalorganic Vapor Phase Epitaxy,” *Thin Solid Films*, 464–465, 244–247, 2004.
- [144] M. S. Arnold, P. Avouris, Z. W. Pan, and Z. L. Wang, “Field-Effect Transistors Based on Single Semiconducting Oxide Nanobelts,” *Journal of Physical Chemistry B*, 107, 659–663, 2003.
- [145] Q. Wan, Q. H. Li, Y. J. Chen, T. H. Wang, X. L. He, J. P. Li, and C. L. Lin, “Fabrication and Ethanol Sensing Characteristics of ZnO Nanowire Gas Sensors,” *Applied Physics Letters*, 84, 3654–3656, 2004.
- [146] C. S. Lao, J. Liu, P. X. Gao, L. Y. Zhang, D. Davidovic, R. Tum-mala, and Z. L. Wang, “ZnO Nanobelt/nanowire Schottky Diodes

- Formed by Dielectrophoresis Alignment Across Au Electrodes,” *Nano Letters*, 6, 263–266, 2006.
- [147] F. Qian, S. Gradecak, Y. Li, C. Y. Wen, and C. M. Lieber, “Core/Multishell Nanowire Heterostructures as Multicolor, High-Efficiency Light-Emitting Diodes,” *Nano Letters*, 5, 2287–2291, 2005.
 - [148] Y. Cui, Q. Q. Wei, H. K. Park, and C. M. Lieber, “Nanowire Nanosensors for Highly Sensitive and Selective Detection of Biological and Chemical Species,” *Science*, 293, 1289–1292, 2001.
 - [149] Y. Huang, X. F. Duan, Q. Q. Wei, and C. M. Lieber, “Directed Assembly of One-dimensional Nanostructures into Functional Networks,” *Science*, 291, 630–633, 2001.
 - [150] Z. H. Zhong, F. Qian, D. L. Wang, and C. M. Lieber, “Synthesis of p-Type Gallium Nitride Nanowires for Electronic and Photonic Nanodevices,” *Nano Letters*, 3, 343–346, 2003.
 - [151] Y. J. Doh, J. A. van Dam, A. L. Roest, E. P. A. M. Bakkers, L. P. Kouwenhoven, and S. De Franceschi, “Tunable Supercurrent Through Semiconductor Nanowires,” *Science*, 309, 272–275, 2005.
 - [152] K. Terabe, T. Hasegawa, T. Nakayama, and M. Aono, “Quantized Conductance Atomic Switch,” *Nature*, 433, 47–50, 2005.
 - [153] B. Z. Tian, X. L. Zheng, T. J. Kempa, Y. Fang, N. F. Yu, G. H. Yu, J. L. Huang, and C. M. Lieber, “Coaxial Silicon Nanowires as Solar Cells and Nanoelectronic Power Sources,” *Nature*, 449, 885–889, 2007.
 - [154] R. C. Hughes, W. K. Schubert, T. E. Zipperian, J. L. Rodriguez, and T. A. Plut, “Thin-Film Palladium and Silver Alloys and Layers for Metal-Insulator-Semiconductor Sensors,” *J. Applied Physics*, 62, 1074–1083, 1987.
 - [155] M. H. Yun, N. V. Myung, R. P. Vasquez, C. S. Lee, E. Menke, and R. M. Penner, “Electrochemically Grown Wires for Individually Addressable Sensor Arrays,” *Nano Letters*, 4, 419–422, 2004.
 - [156] M. Yun, N. V. Myung, R. P. Vasquez, J. Wang, and H. Monboudette, “Nanowire Growth for Sensor Arrays,” *Proceedings of the SPIE Nanofabrication Technologies*, vol. 5220, pp. 37–45.
 - [157] S.-B. Lee, E. Lee, W. Lee, and Y.-C. Joo, “Dendritic Palladium-Silver Nano-Structure Grown by Electrochemical Migration Method for Hydrogen Sensing Device,” *Proceedings of Electronic Components and Technology Conference*, pp. 440–443, 2008.
 - [158] J. A. Paradiso and T. Starner, “Energy Scavenging for Mobile and Wireless Electronics,” *IEEE Pervasive Computing*, 4, 18–27, 2005.

- [159] E. K. Reilly, E. Carleton, and P. K. Wright, "Thin Film Piezoelectric Energy Scavenging Systems for Long Term Medical Monitoring," *Proceedings of the International Workshop on Wearable and Implantable Body Sensor Networks*, pp. 38–41, 2006.
- [160] X. D. Wang, J. H. Song, and Z. L. Wang, "Nanowire and Nanobelt Arrays of Zinc Oxide from Synthesis to Properties and to Novel Devices," *Journal of Materials Chemistry*, 17, 711–720, 2007.
- [161] Z. L. Wang, "Piezoelectric Nanostructures: From Growth Phenomena to Electric Nanogenerators," *MRS Bulletin*, 32, 109–116, 2007.
- [162] Z. L. Wang, "The New Field of Nanopiezotronics," *Materials Today*, 10, 20–28, 2007.
- [163] Z. L. Wang, "Nanopiezotronics," *Advanced Materials*, 19, 889–892, 2007.
- [164] Z. L. Wang, "Zinc Oxide Nanostructures: Growth, Properties and Applications," *Journal of Physics-Condensed Matter*, 16, R829–R858, 2004.
- [165] Z. L. Wang and J. H. Song, "Piezoelectric Nanogenerators Based on Zinc Oxide Nanowire Arrays," *Science*, 312, 242–246, 2006.
- [166] Z. L. Wang, "Towards Self-Powered Nanosystems: From Nanogenerators to Nanopiezotronics," *Advanced Functional Materials*, 18, 3553–3567, 2008.
- [167] M. Alexe, S. Senz, M. A. Schubert, D. Hesse, and U. Gosele, "Energy Harvesting Using Nanowires?," *Advanced Materials*, 20, 4021–4026, 2008.
- [168] Z. L. Wang, "Energy Harvesting Using Piezoelectric Nanowires – A Correspondence on "Energy Harvesting Using Nanowires?" by Alexe et al.," *Advanced Materials, Correspondence*, 20, 1–5, 2008.
- [169] X. D. Wang, J. H. Song, J. Liu, and Z. L. Wang, "Direct-Current Nanogenerator Driven by Ultrasonic Waves," *Science*, 316, 102–105, 2007.



<http://www.springer.com/978-0-387-88782-1>

Electrical Conductive Adhesives with Nanotechnologies

Li, Y.G.; Lu, D.; Wong, C.P.

2010, XII, 437 p., Hardcover

ISBN: 978-0-387-88782-1